Infrared Physics & Technology 60 (2013) 35–55

Contents lists available at SciVerse ScienceDirect

Infrared Physics & Technology

journal homepage: www.elsevier.com/locate/infrared

Review

Infrared thermography for condition monitoring – A review

S. Bagavathiappan, B.B. Lahiri, T. Saravanan, John Philip *, T. Jayakumar

Radiography & Thermography Section (RTS), Non-Destructive Evaluation Division, Metallurgy and Materials Group, Indira Gandhi Centre for Atomic Research, Kalpakkam 603 102, Tamil Nadu, India

HIGHLIGHTS

- Infrared thermography (IRT) is a non-contact condition monitoring (CM) tool.
- We review the advances of IRT for CM of machineries, equipment and processes.
- Applications in various industries are covered in this critical review.
- Basics of IRT, experimental procedures and data analysis techniques are reviewed.
- Sufficient background information for the beginners and non-experts are provided.

ARTICLE INFO

Article history:
Received 2 January 2013
Available online 24 March 2013

Keywords:
Infrared thermography
Condition monitoring
Preventive maintenance
Deformation monitoring
Thermal anomaly
Quality assurance

ABSTRACT

Temperature is one of the most common indicators of the structural health of equipment and components. Faulty machineries, corroded electrical connections, damaged material components, etc., can cause abnormal temperature distribution. By now, infrared thermography (IRT) has become a matured and widely accepted condition monitoring tool where the temperature is measured in real time in a non-contact manner. IRT enables early detection of equipment flaws and faulty industrial processes under operating condition thereby, reducing system down time, catastrophic breakdown and maintenance cost. Last three decades witnessed a steady growth in the use of IRT as a condition monitoring technique in civil structures, electrical installations, machineries and equipment, material deformation under various loading conditions, corrosion damages and welding processes. IRT has also found its application in nuclear, aerospace, food, paper, wood and plastic industries. With the advent of newer generations of infrared camera, IRT is becoming a more accurate, reliable and cost effective technique. This review focuses on the advances of IRT as a non-contact and non-invasive condition monitoring tool for machineries, equipment and processes. Various conditions monitoring applications are discussed in details, along with some basics of IRT, experimental procedures and data analysis techniques. Sufficient background information is also provided for the beginners and non-experts for easy understanding of the subject.

Contents

* Corresponding author. Address: Head, Smart Materials Section, Radiography & Thermography Section, Non-Destructive Evaluation Division, Metallurgy and Materials Group, Indira Gandhi Centre for Atomic Research, Kalpakkam, Tamil Nadu, India. Tel.: +91 044 27480500x26447; fax: +91 044 27480356.
E-mail address: philip@igcar.gov.in (J. Philip).

1350-4495/$ - see front matter
http://dx.doi.org/10.1016/j.infrared.2013.03.006

1. Introduction

The process of monitoring the condition of machineries and processes is called condition monitoring. Condition monitoring aims to prevent unplanned breakdowns, maximize the plant availability and reduce associated hazards. It enables detection of problems before a major malfunction of a machine or component. E.g. The wear and tear of oil and gas pipelines, internal leakages in valves and pressure vessels, etc. can be catastrophic as they can lead to explosions and fire [1]. For aerospace, civil and mechanical engineering infrastructure industries, the process of implementing a damage identification strategy for condition monitoring is known as structural health monitoring (SHM) where damages are defined as changes to the material and geometric properties [2]. Unpredicted failure of machineries and components in industries may result in major accidents and huge economic losses, which warrant regular maintenance of those machineries and components. In large scale industries, the maintenance cost can be as high as 40% of the total budget [3]. Apart from financial losses, poor maintenance of machineries also leads to major accidents which may cause environmental pollution and damage to human lives. Table 1 shows the principal causes behind major accidents [4]. It is evident from the table that mechanical failure causes 38% of all major accidents, which stress the importance of efficient condition monitoring practices. Bragatto et al. observed that, risk based inspection is an essential requirement for sustained operation of critical industrial components [5]. The principal objective of an efficient condition monitoring system is to detect process, component and machine faults, thereby, enhancing the quality of manufactured products and reducing the down time and maintenance cost [6]. Several NDT techniques such as radiography, eddy-current testing, ultrasonic testing, acoustic emission and vibration analysis are routinely used for condition monitoring. It is well known that temperature is one of the most useful parameter that indicates the structural health of an object [7]. Therefore, monitoring the temperature of machineries or a process is undoubtedly one of the best predictive maintenance methodologies. Various temperature measurement systems like thermocouples and resistance temperature detectors (RTD) are in general contact type and does not provide a visual image of the object under investigation. Infrared thermography (IRT) is a novel NDT method that measures the temperature of a body remotely and provides the thermal image of the entire component or machinery. In general, faults associated with abnormal temperature distribution can be easily detected by IRT in advance that allows preventive maintenance before failure.

IRT has been successfully utilized for several condition monitoring applications such as civil structures [8–10], inspection of electrical equipment [11–13], monitoring of plastic deformations [14], inspection of tensile deformation [15–17], evaluation of fatigue damages in materials [18–20], inspection of machineries [21–23], weld inspection [24–27], monitoring of electronic printed circuit boards (PCBs) [28–30] and evaluation of chemical vapor deposition process [31]. IRT has also been utilized in nuclear [32–34], aerospace [35,36], food [37], wood [38], high-level current density identification over planar microwave circuit sectors [39] and paper industries [40,41]. Basics of IRT methodology, operating principle of infrared camera and applications of IRT in building envelope inspection, roof inspection, electrical and mechanical inspection, detection of buried objects, surveillance, process control and condition monitoring of power distribution systems have been discussed in detail by Holst [42]. Applications of IRT for condition monitoring purposes in various fields like nuclear, electrical, PCBs, aerospace, civil, etc. are also described by Reeves [43] and Maldague [44]. Origin of IRT, development of infrared detectors, perspective of IRT applied to building science, application of IRT to thermo–fluid dynamics and combustion systems are well described in a recent book edited by Meola [45]. In this article, we review the applications of IRT in the field of condition monitoring with typical case studies. We also describe the basics of IRT with theoretical background, developments of infrared camera over the last few decades, experimental methodologies and data analysis techniques.

2. Background of IRT and infrared cameras

The origin and theory of IRT has been described in detail elsewhere [46]. For completeness, the basic theory and the fundamental equations are described here. All objects with temperature above 0 K (i.e. −273 °C) emits electromagnetic radiation in the infrared region of electromagnetic spectrum. Infrared radiation (wavelength in the range of 0.75–1000 μm) is positioned in-between microwave and visible part of the electromagnetic spectrum. This vast range can be further subdivided into near infrared or NIR (0.76–1.5 μm), medium infrared or MIR (1.5–5.6 μm) and far infrared or FIR (5.6–1000 μm). In 1800, Sir William Herschel discovered infrared radiation and the recording of the first thermal image was done by his son John Herschel which added new dimension to the temperature measurement. It took almost two centuries to adopt IRT in civilian domain mainly because of non-availability of quality equipment and technical knowhow.

In thermal radiation theory, blackbody is considered as a hypothetical object which absorbs all incident radiations and radiates a continuous spectrum according to Planck's law as follows.

$$L_\lambda = \frac{c_1}{\lambda^5\left[\exp\left(\frac{c_2}{\lambda T}\right) - 1\right]} \quad (1)$$

where λ is the wavelength of the radiation (μm), L_λ is the power radiated by the blackbody per unit surface and per unit solid angle for a particular wavelength (W m^{-2} μm^{-1} sr^{-1}), T is the temperature in absolute scale (K), c_1 and c_2 are the first and second radiations constants respectively. On integrating Planck's law over all

Table 1
Principal causes behind major accidents [4].

Causes	Frequency
Mechanical failure	38
Operational errors	26
Unknown/miscellaneous	12
Process upset	10
Natural hazards	7
Design errors	4
Arson/sabotage	3

Table 2
Wavelength of the peak of the emission spectrum of a typical blackbody at various absolute temperatures.

Temperature (K)	Physical significance	Wavelength of the peak (μm)
3864	Lower limit of infrared region	0.75
1811	Melting point of iron	1.60
1420	Eutectic temperature of iron–carbon	2.04
1000	Eutectoid temperature of iron–carbon	2.89
933	Melting point of aluminum	3.10
373	Boiling point of water	7.77
303	Room temperature	9.56
273	Ice temperature	10.61
77	Liquefaction point of nitrogen	37.63

frequencies, Stefan–Boltzmann's law is derived which is expressed as follows.

$$\frac{q}{A} = \varepsilon\sigma T^4 \tag{2}$$

where q is the rate of energy emission (W), A is the area of the emitting surface (m^2), T is the absolute temperature (K) and σ is the Stefan–Boltzmann's constant ($\sigma = 5.676 \times 10^{-8}\ \mathrm{W\,m^{-2}\,K^{-4}}$) and ε is the emissivity of the emitting surface for a fixed wavelength and absolute temperature T. For a perfect blackbody emissivity is unity, but for real surfaces it is always less than unity. The wavelength of the peak of the emission spectrum is also related to the absolute temperature of the emitting surface by Wien's displacement law, which is expressed as follows.

$$\lambda_{\max} T = 2897.7\ \mu\mathrm{m\ K} \tag{3}$$

Table 2 shows the peak wavelength of the emission spectrum for different ranges of temperatures and the corresponding events. It shows that up to 3864 K the emitted radiation falls within the infrared regions.

In IRT, infrared radiation emitted by a body is detected in a non-contact way by an infrared detector and using Stefan–Boltzmann's law (Eq. (2)), the temperature of the body is obtained. Infrared detectors are the heart of IRT systems. Several types of detectors are available and they can be classified into two main categories, viz. thermal (like pyrometers, bolometers, etc.) and semiconductors (like photoconductive, photovoltaic detectors). Infrared detectors are in general placed inside a protective housing, consisting of the optical arrangements (lens, mirrors, etc.), detector elements, cooling system and associated electronics. Hence, they are also called infrared cameras. Infrared cameras have undergone several modifications during the last few decades [47]. The first generation cameras consisted of a single element detector and two (one horizontal and one vertical) scanning mirrors. In the more advanced second generation cameras two similar scanning mirrors along with array detectors (a large linear array or a small two dimensional array) were used. The modern third generation cameras are without mirrors and have large two dimensional array detectors (popularly known as focal plane arrays: FPA) [48,49]. Several on-chip image enhancement techniques like time delay integration are also implemented in these modern cameras which increase the resolution and sensitivity of the systems. The old technology systems have lower spatial resolution, higher noise levels, smaller dynamic range, limited data storage capabilities and without on-board image processing. Development and basic working principles of various infrared detectors and sensors are described in detail in a book chapter [50].

One of the main advantages of IRT based condition monitoring technique is that it requires minimal instrumentations. The essential requirements for such applications are an infrared camera, a tripod or camera stand and a video output unit for displaying the acquired infrared thermal images. Fig. 1 shows the schematic of a typical IRT experimental setup, where the infrared camera, display unit and a typical infrared image of a mechanical component (compressor motor) along with its original photograph are shown. Nowadays several handheld cameras with built-in display are also available. The benefit of these cameras is that they are light weight and portable. Advances in the field of solid state technology has paved the way for the development of newer types of uncooled infrared detectors with better resolution and accuracy. Presently, thermal sensitivity of the uncooled cameras is about 0.05 °C compared to 0.01 °C of the cooled ones [47].

Several parameters must be considered before choosing an infrared camera as the ability of producing a sharp and accurate thermal image largely depends on these performance parameters. A detailed study of these performance parameters of thermal imaging systems are reported by Venkataraman and Raj [51]. A few important parameters are discussed below.

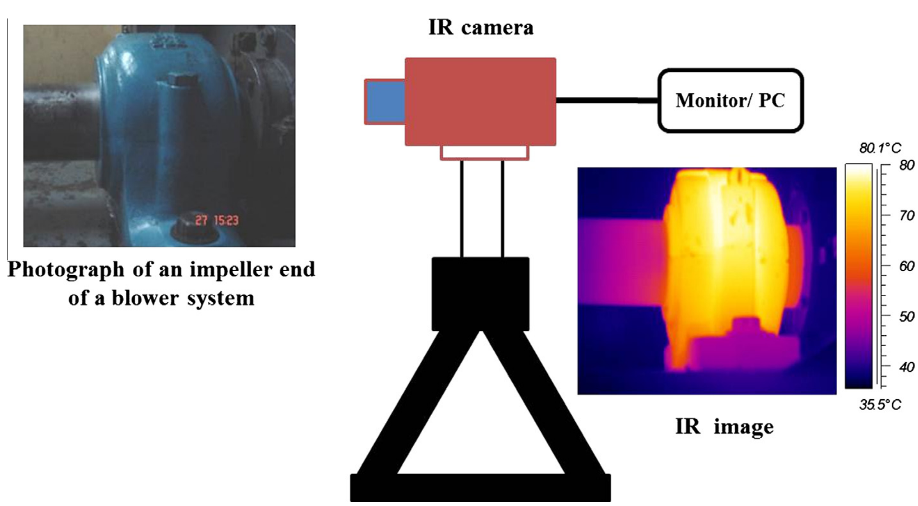

Fig. 1. Schematic of a typical experimental setup for IRT based condition monitoring experiments. The infrared (IR) camera is placed suitably in front of the object under investigation in such a way that unrestricted optical access is available. Environmental conditions must be favorable for accurate temperature measurement. The acquired thermal images are displayed in the personal computer (PC) and real time temperature of the object can be measured in a non-contact way. The acquired thermal images are often pseudo color coded that makes their interpretations easier and faster. The images can also be stored digitally for further post-processing. Here a typical infrared thermal image of a mechanical component along with its original photograph is shown. (For interpretation of the references to color in this figure legend, the reader is referred to the web version of this article.)

Spectral range: Spectral range is defined as the portion of the infrared spectrum in which the infrared camera will be operationally active. As temperature of an object increases, the thermal radiations emitted by the object are more in the shorter wave length bands (this is a direct consequence of Wien's displacement law: Eq. (3)). For observing objects at ambient temperature long wave length band (7.5–14 μm) is preferable. This is because of two reasons, viz. bodies at ambient temperature emits predominantly at these wavelengths and secondly measurements performed at these wavelengths are not affected by the radiation from sun (valid for outdoor measurements), as radiation from sun is predominantly in the shorter wave length bands. Short wave systems (2–5 μm) may be preferred during overcast days and night times [11].

Spatial resolution: Spatial resolution of a thermal imaging system is defined as the ability of the camera to distinguish between two objects within the field of view. A better spatial resolution will result in superior image quality. Spatial resolution of an infrared camera primarily depends on object to camera distance, lens system and detector size. Spatial resolution decreases with increasing object to camera distance. Lens system with small field of view has higher spatial resolution. For example a $10^\circ \times 7^\circ$ lens system has superior spatial resolution than a $20^\circ \times 16^\circ$ lens system. Finally detectors with larger number of array element will produce thermal images with better spatial resolution. For example, 640×512 elements detector will have better spatial resolution than 320×256 elements detector. Typical spatial resolution value for a 320×256 elements detector with $20^\circ \times 16^\circ$ at 1 m object to camera distance will be 1.1 mm/pixel and 1.09 mm/pixel respectively in the horizontal and vertical directions respectively.

Temperature resolution: Temperature resolution is defined as the smallest difference in temperature in the field of view which can be measured by the infrared camera. Temperature resolution depends on several experimental parameters like object temperature, ambient environmental temperature, object to camera distance, presence of filters, etc. The most common parameters used as a measure of temperature resolution are noise equivalent temperature difference (NETD), minimum resolvable temperature difference (MRTD) and minimum detectable temperature difference (MDTD). Though a detailed discussion of these parameters is beyond the scope of the present paper but these quantities are in general determined as per the ASTM standards E 1543-94, E 1213-92 and E-1311-89 respectively. Typical values of NETD for modern Stirling cycle cooled cameras are less than 0.025 K at room temperature.

Temperature range: Temperature range signifies the maximum and minimum temperature values which can be measured using an infrared camera. Typical values are within the range −20 to 500 °C. The range can be extended up to 1700 °C using various filters.

Frame rate: Frame rate is defined as the number of frames acquired by an infrared camera per second. Higher frame rate cameras are in general preferable for monitoring moving objects or dynamic events like propagation of thermal fronts. Typical frame rate values are 50 Hz, i.e. 50 frames per second.

Apart from the above mentioned performance parameters, the selection of an infrared camera also depends on the inherent parameters such as power, size, weight, image processing capabilities, calibration, storage capacity, computer interface, cost and service. Some of the infrared cameras (along with the spectral range, temperature resolution and detector elements) used for condition monitoring applications are presented in Table 3.

3. Experimental methodologies for IRT based condition monitoring

IRT can be broadly classified into two major categories, viz. passive and active. In passive thermography, temperature of the object under investigation is recorded without any external heat stimulation as the object itself acts as a source of heat. Since abnormal temperature distribution over skin surface is a probable indication of illness passive thermography has been extensively used in the field of medical sciences [52–54]. On the other hand, external heat stimulation is essential for active thermography experiments. Depending on the nature of the heat stimulation, active thermography can be further subdivided into several categories like pulsed, lock-in, pulsed phase, etc. [55]. In pulsed thermography, a short duration heat pulse is used as stimulation and the temperature evolution is monitored in the transient domain. Lock-in thermography is performed in the stationary domain, where a sinusoidal heat wave is used as stimulation. Pulsed phase thermography is a combination of both lock-in and pulsed thermography techniques, where data is acquired in time domain but phase analysis is performed in the Fourier domain. Active thermography techniques are in general used for various non-destructive evaluation (NDE) applications like quantification of defects in metallic and composite specimens [56–58], measurement of coating thickness of corrosion protective paints [59] and even in industrial processes [60]. Fig. 2 shows schematic representation of passive and active IRT techniques and related applications. For most of the IRT based condition monitoring applications passive thermography is the preferred experimental technique as experimentation and data analysis is simple and straight forward. Passive thermography is in general used for inspection of civil structures, monitoring of electrical components, machineries, deformation monitoring during tensile and fatigue loading and online weld quality monitoring. External heating is not required for the above mentioned applications as the defective regions appear as hot-spots and significant temperature difference exists between the defect and defect-free regions. On the other hand, in some applications like detection of weld defects (post welding) and inspection of light-weight composite structures of aircraft components external heating is required to induce a significant temperature difference between the defect and defect-free regions and hence, various active thermography techniques are used for such applications. A particular technique is chosen depending on the nature of the object to be inspected, accessibility and expected features of the defect (like size, depth, orientation, and shape).

As condition monitoring experiments are in general performed in shop-floor, plant-site or harsh outdoor experimental conditions, adequate measures are to be adopted to acquire reliable infrared thermal images under these conditions. The factors those are detrimental for an accurate IRT measurement can be classified into three principal categories: procedural, technical and environmental conditions [11]. Procedural factors can be minimized by employing qualified thermographers. A prior knowledge of the object under investigation and experimental conditions enable better thermography images of the object of interest. For example it has been reported that cylindrical specimens can give error in temperature measurement in case of tensile testing due to the restriction of viewing angle of the camera [16]. Technical factors of interest are emissivity of the object under investigation, camera-to-object distance, and load current variation (in case of inspection of electrical equipment) [11,61,62]. Emissivity values play a significant role in determination of correct temperature of an object and caution must be practiced for selecting an accurate emissivity value. In normal day-to-day condition monitoring practices temperature and spectral dependence of emissivity is excluded because they are not substantial. The emissivity values for some materials are listed in Table 4 [42,63]. If possible, the object to inspected is coated with a black-paint (of high emissivity value: $\varepsilon = 0.98$) for enhancing surface emissivity. For example, in case of tensile and fatigue loading or post weld defect detection applications, the specimens are coated with a black paint [26,64]. Avdelidis and

Table 3
Infrared cameras used by different research groups for various condition monitoring applications.

Researchers [Ref.]	Year	Study	Camera used	Detector (spectral range in μm)	Temperature resolution (°C)
Rodgers et al. [126]	1999	Heat transfer predictions in single and multi-component printed circuit boards under natural convection environment	Inframetrics Model 760	HgCdTe (3–12)	<0.2
Clark et al. [9]	2003	Condition monitoring of concrete and masonry bridges	AGEMA Thermovision-900	InSb (2–5.6)	0.1
Venkatraman et al. [64]	2004	Prediction of tensile failure in 316 stainless steel specimens	AGEMA Thermovision-550	PtSi (3.6–5)	<0.1
Speka et al. [203]	2008	Control of laser welding of amorphous polymer	FLIR THERMACAM S40	Uncooled microbolometer (7.5–13)	0.08
Bagavathiappan et al. [21]	2008	Condition monitoring of exhaust system blowers	AGEMA Thermovision-550	PtSi (3.6–5)	<0.1
Wang et al. [143]	2010	Study of necking phenomenon in fiber drawing	FLIR THERMACAM A40M	Uncooled microbolometer (7.5–13)	0.08
Lahiri et al. [26]	2011	Inspection of friction stir weld aluminum and tungsten inert gas welded stainless steel joints	FLIR SC 5200	InSb (2.5–5.1)	<0.025
Fokaides and Kalogirou [109]	2011	Determination of overall heat transfer coefficient (u-value) in building envelopes	FLIR T360	Uncooled microbolometer (7.5–13)	0.06
Naderi et al. [147]	2012	Monitoring dissipated thermal energy and damage evolution of glass/epoxy materials	MIKRON M7500	Uncooled microbolometer (7.5–13)	0.06
Zhang et al. [121]	2012	Monitoring temperature variation of bridge-wires used in electric explosive devices	FLIR A40	Uncooled microbolometer (7.5–13)	0.08

Moropoulou reported that the knowledge of the emissivity values of building materials (like plaster, marbles and porous stones) at various temperatures will reduce the errors in temperature measurement of civil structures [65]. Experiments were performed in two wavelength ranges, viz. 3–5.4 μm and 8–12 μm and it was observed that the emissivity values were closer to unity for the longer wavelength range. In the case of IRT based inspection of metalized top surfaces of some of the integrated circuits (IC), temperature measurement is affected due to the low emissivity values of the metallic components [66]. To avoid the emissivity problem, the temperature of the plastic or ceramic portion alone is considered. Vellvehi et al. developed a new approach for emissivity correction methodology which is based on direct processing of the infrared camera output signal [28]. Environmental conditions also affect IRT measurements in various ways, e.g. an increase in ambient air temperature leads to a higher measured temperature of the objects under investigation, whereas humidity, rain or snow reduces the measured temperature values. Wind-flow and direct solar radiation also affect the measured temperature values of the objects. Studies indicate that apart from emissivity, temperature of civil structures also depends on ambient temperature and relative humidity [67]. It has been reported that high winds can reduce the effectiveness of temperature monitoring of civil structures due to surface temperature shear effects [68]. Standing water on roof, perspex and glass materials must be avoided while using IRT for temperature monitoring of civil structures. In general, IRT based temperature monitoring of large civil structures are performed after sunset to avoid the effects of direct solar radiations and to obtain an appreciable temperature difference between the defect and defect-free regions. As discussed earlier, selection of a long wave length band infrared camera will also be beneficial to reduce the adverse effects of direct solar radiation during day time operations. The experimental methodologies for various condition monitoring applications have been discussed in detail in numerous standards published by different international organizations. A few standards relevant to the field of condition monitoring are enlisted in Table 5. Careful selection of experimental condition along with efficient data analysis procedures can result in high degree of accuracy in IRT based temperature measurement that reduces false alarms and sudden failures.

4. Data analysis methods for IRT based condition monitoring applications

The quantitative analysis of IRT data enables accurate determination of the temperature of a point or a region. On the other hand, in qualitative analysis relative value of a local hot-spot with respect to a reference point is considered. In majority of condition monitoring applications like inspection of electrical components and machineries qualitative data analysis is performed as the methodology is fast and does not warrant rigorous evaluation of the acquired thermal images and provides quick decisions using the difference in temperature of the region of interest and the reference region (ΔT) criteria [11,69]. The severity of the incident is in general represented in terms of ΔT tables, where, three to four different priority classes are present and each class represents a level of severity [70]. Several standards are available, which provide such ΔT tables for qualitative measurement of temperature using IRT for electrical equipment. Some of the commonly used standards are International Electrical Testing Association (NETA) [11,71], American Society for Testing & Materials (ASTM): E 1934-99a [72], National Fire Protection Association (NFPA) [73], military standard: MIL-STD2194 [74] and Allen-Bradley motor control center standard [75]. Infraspection institute standard specifies the experimental methodologies and data analysis techniques for electrical components as well as rotating components [76]. Maximum allowable temperature of several mechanical components (like bearing, rolling elements, lubricants, grease, synthetic coils, seals, gaskets, gear drives, chain drives, etc.) are listed in this standard. Under normal operational conditions temperature of a particular component must not rise beyond the maximum allowable value enlisted in the above mentioned standard. Table 6 shows the salient features of the NETA, MIL-STD2194 and

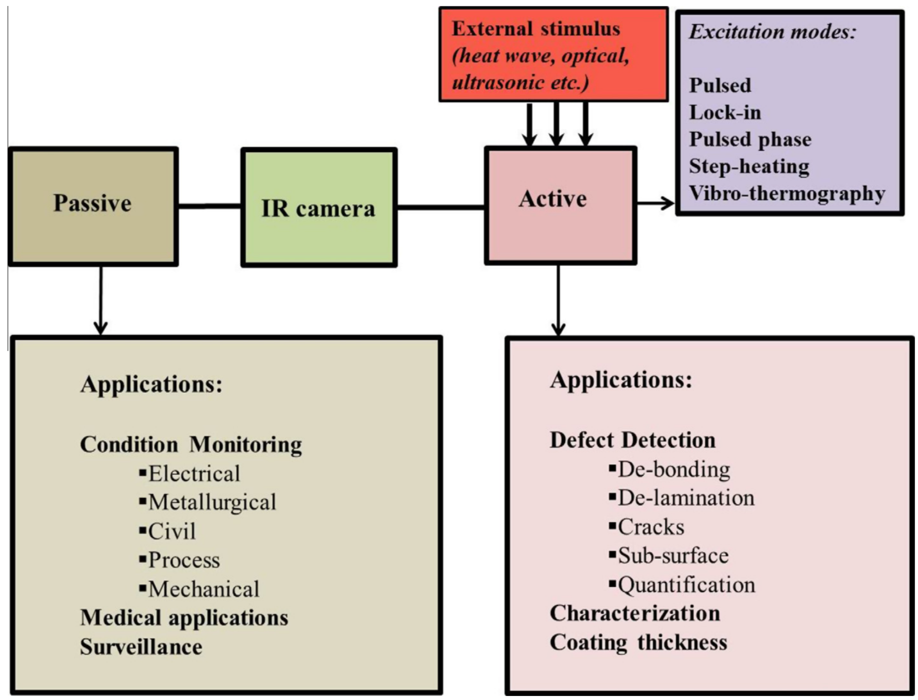

Fig. 2. Schematic representation of passive and active thermography techniques along with various applications. External heating is not required for passive thermography, whereas active thermography requires adequate external heat stimulation like heat wave, optical, ultrasonic, etc. Depending on the mode of stimulation active thermography can be further subdivided into pulsed (short duration heat pulse is used), lock-in (sinusoidal heat wave is used), pulsed-phase (combination of pulsed and lock-in), step heating (long duration heat pulse), vibrothermography (heat generated by ultrasonic excitation), etc.

Table 4
Emissivity of some common materials [42,63] (when wavelength is not specified, it covers the entire MIR and FIR range).

Materials	Temperature (K)	Wavelength (μm)	Emissivity
Aluminum (heavily weathered)	290	–	0.83–0.94
Asbestos	293	–	0.96
Brass (polished)	301	–	0.03
Cast iron (heavy oxidation)	377	–	0.95
Cement	298	8–14	0.54
Clay (fired)	298	8–14	0.91
Common brick	290	2–5.6	0.81–0.86
Concrete (dry)	309	5	0.95
Copper (oxidized)	311	–	0.87
Fiberglass	293	–	0.75
Granite (natural surface)	309	5	0.96
Graphite	293	–	0.98
Limestone	311	–	0.95
Marble (gray, polished)	311	–	0.75
Masonry brick	273	5	0.94
Mica	311	–	0.75
Mortar (dry)	311–533	2–5.6	0.94
Nickel (polished)	298	3–14	0.05
Tempered iron (polished)	313–523	–	0.28

Infraspection institute standards. As qualitative monitoring suffers from several drawbacks like non-availability of standard data tables and lack of accuracy, detection of systematic equipment failures requires rigorous quantitative analysis [11].

Infrared thermal images are in general noisy and suffer from low signal to noise ratio. Hence, various image processing techniques are used for enhancement of the acquired thermal images. From condition monitoring point of view the principal objectives of image processing are detection of hot-spots and extraction of defect features. For image enhancement purposes various point operation algorithms like contrast stretching, histogram equalization, etc. can be used. The objective of these algorithms is to stretch the histogram of an image, which will in turn increase the dynamical range of the image, thereby enhancing the contrast. Using advanced signal analysis techniques like thermographic signal reconstruction (TSR) and principal component analysis (PCA) defects of greater depths can be detected with higher thermal contrast [77]. The texture analysis based feature extraction of thermal images has been found to be helpful in image classification and object shape determination [78]. For detection of hot-spots image segmentation and image thresholding are performed. Several segmentation and thresholding algorithms are used and their choices depend on the nature of the image and the objective of the users. The most commonly used segmentation and thresholding algorithms are global thresholding [57], fuzzy thresholding [79], morphological segmentation [69,80], two level segmentation [81]

Table 5
Relevant standards for condition monitoring applications.

Sl. no.	Standard reference no.	Topic	Title of the standard
1	ASTM-E1213-97	Temperature resolution	Standard test method for minimum resolvable temperature difference for thermal imaging systems
2	ASTM-E1311-89	Temperature resolution	Standard test method for minimum detectable temperature difference for thermal imaging systems
3	ASTM-E1543-00	Temperature resolution	Standard test method for noise equivalent temperature difference of thermal imaging systems
4	ASTM-E1862-97	Temperature correction	Standard test methods for measuring and compensating for reflected temperature using infrared imaging radiometers
5	ASTM-E1933-99a	Emissivity correction	Standard test methods for measuring and compensating for emissivity using infrared imaging radiometers
6	ANSI/IEEE C37.010-4.4.3	Electrical inspection	IEEE application guide for AC high-voltage circuit breakers rated on a symmetrical current basis
7	ASTME1934-99a	Electrical and mechanical inspection	Standard guide for examining electrical and mechanical equipment with infrared thermography
8	ISO 18434	Mechanical inspection	Condition monitoring and diagnostics of machines-thermography
9	ISO-18436-8	Mechanical inspection	Condition monitoring and diagnostics of machines — requirements for training and certification of personnel-thermography
10	IS 12782	Industrial inspection	Guidelines for using thermography for monitoring of industrial components
11	ASTM-E2582-07	Aerospace industry	Standard practice for infrared flash thermography of composite panels and repair patches used in aerospace applications
12	ASTM-D4788-03	Civil inspection	Standard test method for detecting delaminations in bridge decks using infrared thermography
13	EN 13187	Building inspection	Thermal performance of buildings. Qualitative detection of thermal irregularities in building envelopes – infrared method
14	ASTM C1046-95	Building inspection	Standard practice for in situ measurement of heat flux and temperature on building envelope components
15	ASTM C1060-11a	Building inspection	Standard practice for thermographic inspection of insulation installations in envelope cavities of frame buildings
16	ASTM C1153-10	Building inspection	Standard practice for location of wet insulation in roofing systems using infrared imaging
17	ISO 6781	Building inspection	Thermal insulation – qualitative detection of thermal irregularities in building envelopes – infrared method
18	ISO 13790	Building inspection	Annual energy use for heating and cooling of the building

and normalized cut segmentation [82]. It has been reported that ground truth segmentation technique is best suited for infrared images [11]. In many condition monitoring application edge detection filters are used for isolating the boundary of a particular defect [83]. Various types of edge detection filters (like Sobel, Canny, Prewitt, etc.) are in use and again the choice of a suitable edge detection filter depends on the nature of the image and user-objective. A detailed discussion on various image processing techniques is beyond the scope of the present paper and several dedicated books are available on this subject [84]. Various image processing techniques suitable for condition monitoring application have been discussed in detail in a recent review authored by Jadin and Taib [11]. Fig. 3a shows a typical infrared thermal image of a PCB with two faulty integrated circuit (IC) components, which show higher temperature compared to the surrounding regions. The faults could be easily visualized in the histogram equalized image shown in Fig. 3b. Application of image processing tools will lead to intelligent image analysis system which will ultimately pave the way for automated fault detection and localization systems. Such automatic inspections techniques for infrared thermal images have already found widespread applications in the medical [52,85] and NDT [86,87] fields.

5. Applications of IRT in condition monitoring

Faulty machineries, improper electrical loading conditions, damaged metallic or non-metallic components in general present abnormal temperature patterns. Further, temperature is one of the most important controlling parameters in various industrial processes. Identification of abnormal temperature patterns and online temperature measurement performed in a non-contact way using IRT assist early diagnosis of the probable faults and proper preventive measures can be adopted to avoid major shutdowns. Thermographic findings are often compared with the results obtained from other techniques like ultrasonic inspection, vibration analysis, etc. for versatile multi-mode condition monitoring to ensure reliability and accuracy. Fig. 4 shows a few applications of IRT in condition monitoring like monitoring of machinery, liquid level monitoring, inspection of PCBs, condition monitoring of transformer circuit breakers, motor shaft belt and three phase electrical connections. The benefits of IRT are that it is remote, non-contact and non-invasive technique that enables simultaneous monitoring of a large area. Also IRT enables recording of dynamical variations of temperature in real time and interpretations of the acquired pseudo color coded infrared thermal images are easier and faster. Based on the measured temperature values, proper decisions can be made about the maintenance and repairing schedules. Thus, IRT helps to reduce equipment damage, system down time and maintenance cost. Due to these advantages, IRT has been established as an effective condition monitoring tool. A few applications of IRT in condition monitoring in various domains along with suitable case studies are discussed in detail below.

5.1. Monitoring of civil structures

Concrete structures such as bridges, roadways, water and sewer systems, ports, harbors, airports and buildings are integral parts of our lives and in-service condition monitoring of these structures are essential to ensure public safety. Buyukozturk compared various concrete imaging techniques and concluded that IRT can be used for remote, rapid and accurate imaging of the concrete structures [88]. He also indicated that accurate imaging of concrete needs additional requirements due to its heterogeneous composition, variable grain size distribution and different properties of the constituent materials. The other constrains include complex physical geometries, restricted accessibility and existence of reinforcement. The application of IRT in detection of voids and cracks, detachment of frescos, wall bonding, moisture entrapment and analysis of heating–ventilating–air-conditioning (HVAC) systems

Table 6
Salient features of NETA and MIL-STD2194 standards for IRT based inspection of electrical equipment [11,71,74,76].

Standards	Temperature difference (ΔT) (°C)		Recommended action
NETA	Between similar components under identical loading	Between components and ambient air temperature	
	1–3	1–10	Possible deficiency, warrants investigation (priority: 4)
	4–15	11–20	Indicates probable deficiency, repair as time permits (priority: 3)
	–	22–40	Monitor continuously until corrective measures can be accomplished (priority: 2)
	>15	>40	Major discrepancy, repair immediately (priority: 1)
MIL-STD2194	10–20		Component failure unlikely but corrective measures required at next scheduled routine maintenance period
	24–40		Component failure probable unless corrected
	40–70		Component failure almost certain unless corrected
	>70		Component failure imminent
Infraspection institute standard for electrical and/or mechanical components	1–10		Corrective measures should be taken at the next maintenance period
	>10–20		Corrective measures required as scheduling permits
	>20–40		Corrective measures required ASAP (as soon as possible)
	>40		Corrective measures required immediately

are described in detail in a recent book chapter authored by Grinzato [89]. Ljungberg described various civil applications of IRT like indoor and outdoor thermography of buildings, heating networks, sewer systems, wastewater pipes, roads, bridges, asphalt paving, canals, etc. [90]. Clark et al. used IRT for diagnosis of civil structures under low ambient temperature conditions and reported that, the temperature difference between the delaminated and normal areas could be about 0.2–0.3 °C [9]. Datcu et al. proposed a method, using highly reflective and diffusive aluminum mirror, to improve the IRT based temperature measurement for inspection of civil structures [91]. Meola used IRT for inspection of single and multi-layered masonry structures [10]. The data was reduced to two dimensionless quantities, viz. D_T (related to induced defect thermal effects) and D_e (related to the characteristics of the defect and host material). It was observed that a power law relationship exist between D_T and D_e. Maierhofer et al. applied impulse thermography technique for detection of subsurface voids in concrete structures and studied the effect of concrete age, pore content, aggregate type, reinforcement density and hydration level in detail [92]. Studies indicate that IRT can be used for condition monitoring of facades, investigation of interfaces between plasters and masonry, crack detection, inspection of the structure of mortar filling of joints and detecting sub-surface moisture [93]. Poblete and Pascual used active thermography for measurement of concrete porosity which ultimately affects the durability of the concrete [94]. Azenha et al. used IRT for monitoring early age hardening of concrete [95]. The authors indicated that temperature monitoring during concrete casting is essential to avoid thermal cracking and using IRT can be beneficial for this purpose, as temperature evolution over a large surface area can be visually monitored in a non-contact way. Arndt used pulsed phase thermography technique for studying subsurface defects in civil structures [96].

IRT has also been widely used for condition monitoring of ancient structures of historical and cultural importance. Grinzato et al. used IRT for monitoring hidden wall structures and moisture content in ancient buildings [97]. Studies indicate that IRT can be used as a powerful tool for studying the structural integrity of the ancient monuments, air flow pattern, adhesion properties of frescos and for detecting cracks [8]. Avdelidis and Moropoulou used IRT for investigation of historical structures after conservation or restoration work and concluded that, IRT can be considered as a powerful tool for condition monitoring and evaluation of conservation status of such structures [98]. Tavukcuoglu et al. used IRT for diagnosis of surface water drainage problems in historical buildings [99]. Their studies show that underground drainage path and pipeline could be detected using IRT and rising damp problems were in general associated with inadequate site grinding and reverse falls near the problematic regions. Luong applied IRT for studying soil dynamics, especially the energy dissipating ability of soil and concluded that IRT could be used for directly monitoring the stress state of particle rearrangement and to observe the fuse effect of soil which significantly reduces the earthquake loading on civil engineering structures [100]. Sugiura et al. used IRT for monitoring ground water status [101]. Thermal images were acquired from a low altitude helicopter and atmospheric correction

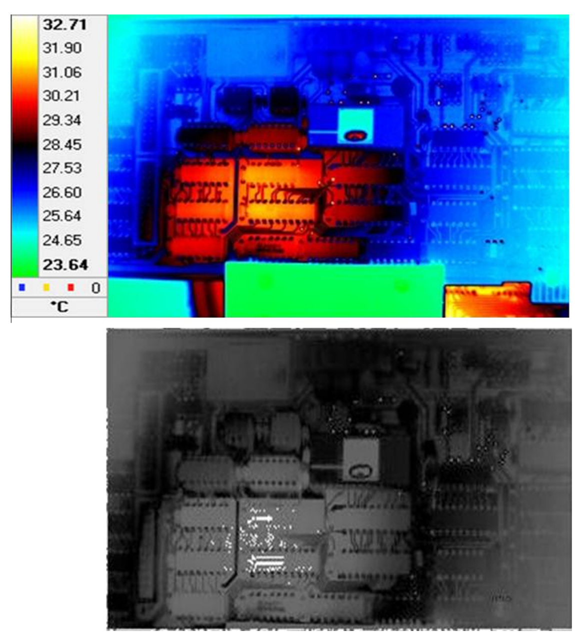

Fig. 3. (a) Infrared thermal image of a printed circuit board (PCB) with typical faults due to malfunctioning of integrated circuit (IC) components. The faulty regions have higher temperature compared to the normal regions. (b) Output image of the histogram equalization operation on the original image (Fig. 4a). The histogram equalized image provides better insights into the fault location and may help in fault classification. Application of such image processing techniques will result in the development of automated fault recognition systems which will ultimately lead the way for robust, reliable and accurate intelligent condition monitoring methodology.

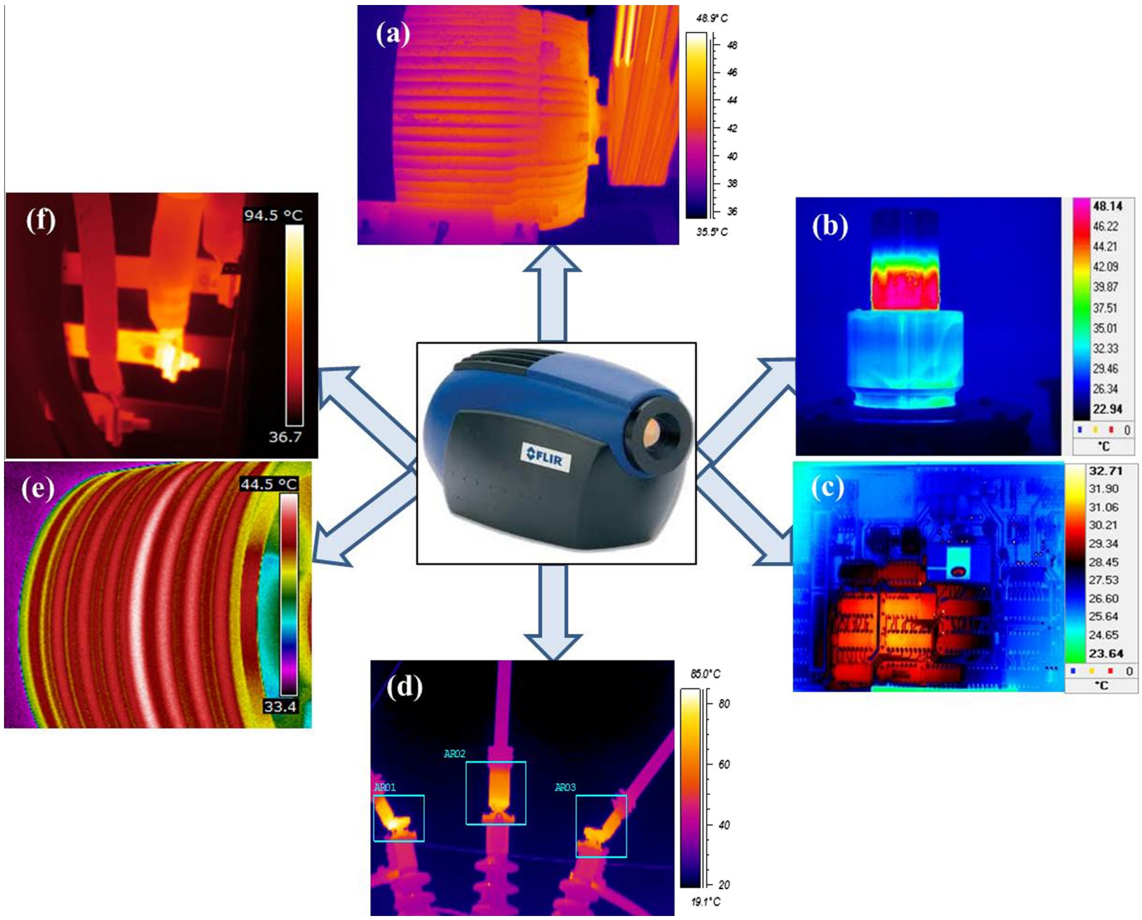

Fig. 4. Various condition monitoring applications of infrared thermography: (a) Monitoring of machineries where abnormal surface temperature distribution is an indication of a probable flaw. (b) Inspection of liquid levels in industrial components. (c) Inspection of printed circuit boards. Localized defects like short circuits or current leakages produce hot-spots which can be easily detected by infrared thermography. (d) Typical thermal images of a transformer circuit breaker where the faulty regions can be clearly seen as hot-spots. (e) Inspection of shaft belt where the thermal anomaly is due to over-tightening of a belt. (f) Condition monitoring of three phase electrical panel where local hot spots are developed due to load imbalance.

was performed on the acquired thermal images. The authors concluded that IRT can be considered as a useful tool for determination of soil moisture status. Vavilov and Demin used IRT for monitoring the operation of smokestacks [102].

Nowadays performance indicators for new and existing building are derived from the temperature patterns and IRT can be used for studying thermal insulations of such civil construction remotely [89]. In 2006 it was made obligatory for salesman to perform IRT based thermal balance inspections of houses at the point of resale in France [103]. Residential energy services network (RESNET) has published several standards for energy auditing of residential buildings, which discusses the important technical guidelines and energy rating of the buildings [104]. Balaras and Argiriou used IRT for detection of energy leakages from building envelopes [105]. They indicated that IRT can be used for detection of heat losses, missing or damaged wall insulation, air leakages and trapped moisture. Their studies also indicated that a temperature difference of about 11 °C between the interior and exterior surface may be a possible indication of missing or damaged insulation. Sales et al. studied the thermal performance of expanded polystyrene (EPS) as insulators using IRT [106]. Ludwig developed a simplified heat transfer model for the civil buildings and the same was verified using IRT [107]. Haralambopoulos and Paparsenos used IRT for monitoring the level of thermal insulation in old buildings and for detecting heat leakages in the building envelopes [108]. Fokaides and Kalogirou used IRT for determining the overall heat transfer coefficient (u-value) for building envelopes during summer and winter time [109]. Their findings were confirmed using thermohygrometry and the authors concluded that IRT may be a more accurate technique as it incorporates radiative heat transfer and surface emissivity. A typical infrared thermal image of a residential building acquired during night time is shown in Fig. 5 [110]. Red color denotes the hotter regions whereas, blue denotes the cooler regions. It is clearly seen that heat loss is mainly through the doors and the windows. Fig. 6a shows the photograph of a plastered wall of an ancient chapel showing some cracks, and Fig. 6b and c shows the thermal image and phase image of the same wall respectively [93]. It can be seen from the phase image that the positions of the cracks are mainly inside the joints and between the bricks. The above mentioned case studies clearly indicate the effectiveness of IRT as a condition monitoring tool for civil inspections. IRT can be used for detection of voids and cracks, delaminations, loss of insulation, energy loss from a building and even for evaluation of damage and repair of ancient civil structures of cultural importance.

5.2. Monitoring of electrical and electronic components

IRT has found widespread applications in condition monitoring of electrical components. Corrosion, loose connection, damaged contacts, worn out wires, over loading or load imbalance are the major types of faults in electrical components that causes abnormal rise of temperature which can be easily monitored by IRT. The operating temperature of typical electrical equipment under normal load condition may be considered as the baseline data and any increase in operating temperature must be considered as an indication of a probable fault. In general, product manufacturers or international associations like IEEE, ANSI, IEC publish the normal temperature ratings of electrical equipment which can be compared with the measured temperature values for condition monitoring purposes [13]. Newport classified the common causes of electrical faults into four main categories, viz. increased resistance (localized resistance due to deterioration of electrical contacts over time or over tightening of bolts), load (I^2R heating or Joule heating, where I is the electrical current and R is the resistance), induced heating (eddy current heating in metallic specimens) and harmonics (multiples of basic incoming frequency; odd harmonics or triplens are reported to be most harmful and may cause severe overvoltage, over current or overheating) [111]. Martinez and Lagioia classified the major sources of electrical faults into three sections based on the case studies during the period 1999–2005 [112]. They reported that maximum numbers of faults (48%) were found in connection accessories and bolted connections, whereas 45% of faults were found to be in disconnector contacts. They classified the fault induced thermal anomalies into three categories and also recommended suitable preventive procedures for each category. The three categories are serious (overheating >130 °C), priority (overheating 100–130 °C) and programmed (overheating 75–100 °C). For serious types of faults repair and maintenance work should commence immediately, whereas, for priority and programmed type of faults repair and maintenance work can be taken up as soon as possible and when possible respectively. The following formula may be applied while using the ΔT criteria (described earlier) to obtain the corrected maximum allowable temperature ($T\max_{\mathrm{Corr}}$ in °C) [76,113].

$$T\max_{\mathrm{Corr}} = \left[\left(\frac{A_M}{A_R}\right)^2 T_R\right] + T\mathrm{amb}_{\mathrm{M}} \tag{4}$$

Here A_M, A_R, T_R and $T\mathrm{amb}_{\mathrm{M}}$ are the measured load in amperes, rated load in amperes, rated temperature rise obtained from standards (°C) and measured ambient temperature (°C) respectively.

Hurley described the applications of IRT for condition monitoring of oil submerged high resistance equipment, transmission systems, heavily insulated connections, lighting arrestors and underground lines [114]. Studies by Epperly et al. concluded that

Fig. 5. A typical infrared thermal image of a residential building acquired during night time [110]. Red color denotes the hotter regions whereas, blue denotes the cooler regions. It is observed that heat loss is mainly through the doors and the windows. This image clearly demonstrates the applicability of infrared thermography as a potential tool for assessing energy losses of buildings. (For interpretation of the references to color in this figure legend, the reader is referred to the web version of this article.)

IRT can be used for condition monitoring of various types of electrical equipment like motor control centers, transformers, substation and switchgears, capacitor banks, overhead power lines, drives, light and power panels, power cables and trays, terminal strips and power supplies [115]. Showalter and Edmonds used thermal maps generated from thermal scanners for detecting in-service winding failure of newly installed replacement hydro-generator stators [116]. Ralph highlighted the application of IRT in condition monitoring of high and low voltage transformers, radiator type cooling fans of oil-filled transformers, high tension tower connection lines, exciter rectifiers and oil filled circuit breakers [117]. Frate et al. used IRT for performance monitoring of overhead lines and joints [118]. Bonin used IRT for inspecting loose connections in high tension grid system and a synchronous motor of a hydrocarbon compressor [119]. Chudnovski used IRT to inspect the corrosion induced overheating of electrical components which is a very common cause for fire and safety hazard in pulp and paper industries [120]. Zhang et al. used IRT for studying the temperature variation of bridge-wires (widely used in electric explosive devices as transducers of electrical energy to thermal energy) under constant current operating conditions [121]. They reported that application of IRT can help to predict the safety current values for bridge-wires of different diameters. Filho and Henriquez successfully used IRT in high-level current density identification over planar microwave circuit sectors [39]. Wang et al. used IRT for inspecting cooling system blockage and connection flaws in power transformers [122]. The authors categorized the severity of the flaw induced overheating into four types, viz. attention, intermediate, serious and critical depending on the temperature rise of 0–9, 10–20, 21–49 and >50 °C respectively. Fig. 7a and b shows the normal photograph and typical infrared thermal image of a 225 MV A transformer respectively [123]. The heat generation in the transformer can be clearly seen from the thermal image. IRT based condition monitoring of electrical equipment can significantly reduce unplanned shutdown, maintenance time and risk of accidents and fire hazards.

Recent progress in the field of integrated circuits and solid state technology has resulted in the widespread usage of printed circuit boards (PCBs) containing millions of electronic circuits. Such high density packing requires usage of multiple on board power supplies and numerous electronic junctions which are potential sites of faults. Identification and localization of such faults is essential for error free performance of the PCBs. In general, the faults produce abnormal temperature patterns which could be detected by IRT. Recent usage of non-lead solders with high melting point may result in additional temperature load for the electronic circuits and IRT can be used for real-time temperature monitoring in such cases [124]. Dumpert discussed the IRT based methodologies for inspecting PCBs in detail [66]. Several testing procedures like batch screening, low volume screening, single piece fault localization, etc. are illustrated with suitable case studies. Vishwakarma et al. reported that temperature rise at the various locations of a PCB can be recorded using IRT and the fault can be easily detected from the thermal anomalies [125]. IRT has been used for experimental validation of the numerical heat transfer problem of the PCBs under natural and forced convection cooling conditions [126–128]. Wiecek et al. used transient active thermography techniques for the estimation of solder thickness in PCBs [129]. The solder thickness values were extracted from the observed transient temperature patterns. Avdelidis et al. used pulsed thermography technique for defect detection in the PCBs [124]. Gupta et al. used IRT for diagnosis of defects in the thermal interface materials of the integrated heat spreaders in advanced microprocessors [130]. They observed that internal die heating yielded better results compared to the traditional external transient excitations. Breitenstein et al. developed a microscopic lock-in IRT technique for inspection of

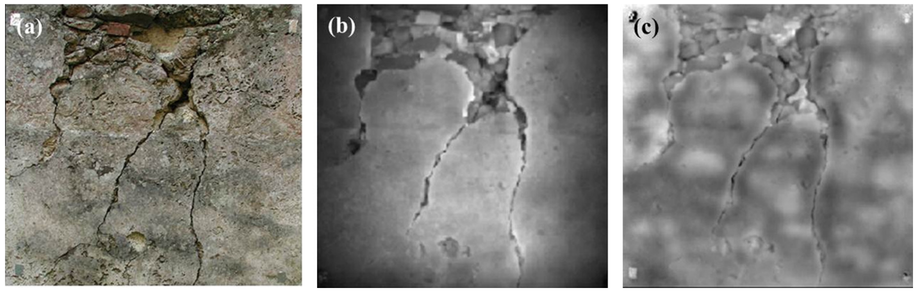

Fig. 6. Condition monitoring of civil structures using infrared thermography [93]. (a) Photograph of a plastered wall of an ancient chapel showing some cracks. The region was heated with an infrared radiator for 10 min and during cooling, thermal images were acquired at 5 Hz frame rate for 45 min. (b) Infrared image just after the heating was stopped. The cracks and the associated regions can be clearly seen. (c) Phase image obtained from pulsed phase thermography technique. Single stones appeared as lighter areas; on the other hand joint stones appeared as darker regions. It can be seen from the phase image that the positions of the cracks are mainly inside the joints and between the bricks.

leakage sites in the ICs [131]. Temperature difference as low as 10 μK and spatial resolution of about 5 μm have been achieved by using this technique. Studies indicate that 1 mA of leakage current could be localized within a few seconds, whereas it took less than an hour for detection of a few μA of leakage current [29]. From the above mentioned case studies it is clear that IRT can be considered as a sensitive, reliable and easy to use condition monitoring technique for fault identification in PCBs. IRT based method for fault localization in electronic assembly can ensure quality control during the PCB fabrication and population stages.

5.3. Deformation monitoring

Material can experience various types of loading conditions during operation which can drastically reduce its service life. Tensile or fatigue loading causes deformation in components and part of the mechanical energy is converted to thermal energy which in turn increases the component temperature. Deformation induced heat generation can be represented by the generalized heat conduction equation [132].

$$\rho C\left[\frac{\partial T}{\partial t} + v grad(T)\right] - div[k grad(T)] = S_e + S_i \qquad (5)$$

where ρ is the mass density, C is the specific heat, k is the heat conduction tensor, T is the absolute temperature, v is the velocity field, S_e is the external volumetric heat source and S_i is the internal volumetric heat source (like thermoelastic effect, intrinsic dissipations, etc.) respectively. IRT is an excellent technique for monitoring the surface temperature evolutions during such deformations and provides early indications of failure. IRT can provide early indication about the zone of failure during tensile loading [64]. Wang and Zhang studied the necking phenomenon in metallic specimens under uniaxial tensile loading experimentally using IRT and also using finite element modeling [133]. IRT has been used for monitoring tensile deformation in nuclear grade AISI type 316 stainless steel (SS) at room temperature [15]. It was observed that temperature increases continuously during progressive plastic deformation and the onset of necking can be clearly identified by the sudden increase in temperature at the necking region. Rodriguez-Martinez et al. used IRT for studying martensitic transformation in AISI 304 SS specimens under tensile loading at room temperature [134]. They observed that under macroscopic low strain rate experimental conditions, martensitic transformation occurred for temperature difference greater than 140 °C. Oliferuk et al. studied the elastic to plastic transition under uniaxial tensile loading in austenitic steel, titanium and aluminum alloys [135]. They observed a decrease in specimen temperature followed by an increase under such transition. This study concluded that the temperature inversion point is an indication of initiation of plastic deformation over macroscopic scales and IRT is a valuable tool for such measurement due to its fast response in temperature measurement. The effect of stress triaxiality on material deformation studied in smooth as well as axisymmetrically notched specimens of IMI-834 titanium alloy using IRT indicated that the localized temperature rise was higher in case of the notched specimens compared to the smooth ones [16]. It has been shown that the stress in the thermoelastic region can be predicted from the temperature data using the Lord Kelvin's equation as described below.

$$\Delta T = -K_m T \Delta\sigma \qquad (6)$$

where ΔT is the change in temperature (K), T is the specimen temperature (K), $\Delta\sigma$ is the stress change (Pa) and K_m is the thermoelastic coefficient and is expressed as

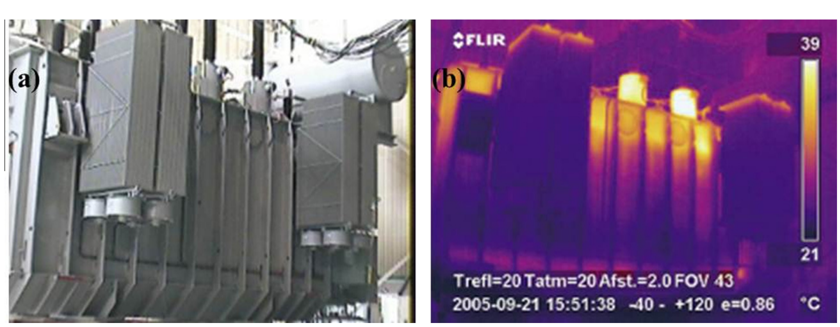

Fig. 7. Infrared thermography is routinely used for condition monitoring and preventive maintenance of electrical transformers [123]. (a) Photograph of a 225 MV A transformer. (b) Typical infrared thermal image of the transformer shown in Fig. 7a under operational conditions. The heat generation in the transformer can be monitored remotely and any unnatural increase in temperature, which can be an indication of a probable fault, can be inspected beforehand. This increases the efficiency of the transformer, reduces down-time and saves maintenance cost.

$$K_m = \frac{\alpha}{\rho C_P} \tag{7}$$

where α is the coefficient of linear expansion (m K^{-1}), ρ is the density (Kg m^{-3}) and C_P is the specific heat at constant pressure (J $kg^{-1}K^{-1}$). Kutin and Adamovie used IRT based methodology for deformation monitoring in butt welded joints of S355J2G3 steel specimens during tensile loading [136]. Badulescu et al. used IRT and grid method for studying plastic deformation in aluminum multi-crystal specimens under tensile loading and observed that heat sources estimated from the acquired temperature data matches well with the strain distribution [14]. Louche and Chrysochoos used IRT for studying Luders band propagation in S355MC steel specimens during displacement controlled tensile test and observed a low amplitude thermal wave propagation which was attributed to the Luders band propagation [132]. Ranc and Wagner studied the heterogeneous deformation related to Portevin–Le Chatelier (PLC) bands in an aluminum–copper alloy system using IRT and concluded that IRT can be used for quantification of deformation increment [137]. Ait-Amokhtar et al. studied the dynamics of PLC band formation in an aluminum–magnesium alloy system under constant strain rate tensile loading and found that the acquired temperature data provides information about formation and movement of various PLC bands [17]. Type A PLC bands were formed under large strain rate and their propagation was found to be quasi-adiabatic. On the other hand, under low strain rate conditions, type B PLC bands with quasi-isothermal propagation were formed. Their studies indicated that the strain rate jumps can be quantified from the measured temperature bursts. It has been reported that IRT can be used for studying transition from continuous (type A) PLC bands to discontinuous (type B) PLC bands [138]. Studies show that heat production due to phase transitions in shape memory alloys can also induce measurable changes in temperature [139]. IRT has been used for detecting phase transformations in shape memory alloys during mechanical testing [140]. Delpueyo et al. applied IRT for studying martensitic microstructures in a shape memory alloy during cyclic loading [141]. IRT has also been used for deformation monitoring of non-metallic specimens like rubber and fiber. Wang et al. used IRT for studying the thermal effects on rubber specimens during loading–unloading cycle [142]. Their studies indicate that thermoelastic effect could be observed during the loading cycle and temperature variations were partly reversible in the first cycle and totally reversible in the subsequent cycles due to complex deformation behaviors. Wang et al. studied necking phenomenon during fiber drawing process using IRT [143]. It was observed that the temperature exponentially increases with fiber drawing rate. Meola and Carlomagno studied impact damages in glass fiber reinforced polymer (GFRP) using IRT and reported that online monitoring of impact testing is useful for material characterization [144]. It was observed that for impact energy below 7 J, the material exhibited only elastic response (characterized by a sudden decrease in temperature followed by a quick recovery to ambient temperature). On the other hand for impact energy beyond 7 J hot-spots were observed which signified the initiation of damage in the material. It was further observed that the damage locations coincided with the location of onset of heat generation.

Fargione et al. used IRT for observing temperature evolutions during fatigue testing of materials and reported that this technique is suitable for rapid determination of fatigue curves [145]. Rosa and Risitano used IRT for to determine fatigue limit by analyzing the temperature of the external surface during cyclic loading [146]. The method is based on the increase of surface temperature for stress levels beyond fatigue limit of the materials. Luong indicated that IRT can be used for inspection of fatigue induced damage processes, early detection of the intrinsic dissipation and rapid evaluation of fatigue strength of materials [18]. IRT is a potential experimental tool for determination of intrinsic dissipation during deformation. Naderi et al. studied the heat dissipation in a glass/epoxy laminate which was subjected to bending fatigue loading [147]. They observed that the dissipated thermal energy can be estimated by analyzing the surface temperature and rate of temperature fall (after sudden halting of fatigue loading). Maquin and Pierron studied various visco-elastic and micro-elastic effects during fatigue loading using IRT [148]. Pastor et al. studied the low cycle fatigue behavior of 2024-T3 aluminum alloy using IRT and observed temperature oscillations due to thermoelastic coupling [19]. The study concluded that transient loading to stress level higher than the yield stress of the test material causes sudden increase in temperature which can be measured by IRT. Giancane et al. used IRT for studying the high cycle fatigue behavior of 2024-T3 aluminum alloy [149]. Ummenhofer and Medgenberg applied IRT for analysis of localized fatigue damages during fatigue testing of manual arc welded S355J2G3 steel components [150]. They reported that IRT is a valuable tool for determination of fatigue damage initiation and localized inhomogeneous damages can also be identified since temperature data over a wide area which covers the entire specimen can be acquired using IRT. Studies indicate that IRT can be used for analyzing the heat sources associated with fatigue process of 2024-T3 aluminum alloy and zones with higher thermoelastic source amplitude can cause the onset of fatigue cracks [151]. Plekhov et al. found that spatial standard deviation (SD) of temperature data acquired by IRT can be used for monitoring fatigue crack initiation and current location of the crack tip [152]. Fig. 8 shows the infrared thermal image of fatigue testing of reactor pressure vessel steel SAA533B1I2 [153]. Fig. 8a and b shows the temperature distribution of the specimen after 280,000 and 285,000 cycles respectively and Fig. 8c shows the subtracted image where the location of the fatigue crack tip region can be clearly seen. It is evident from the above case studies that IRT is an excellent tool for deformation and damage monitoring of metallic as well as non-metallic components. Degradation of material properties can be remotely monitored and sudden catastrophic failures can be avoided using IRT based condition monitoring.

5.4. Inspection of machineries

IRT has been widely used for condition monitoring of machineries [154]. Stator or rotor misalignments, faulty bearings, improper lubrication may cause major mechanical failures unless proper preventive monitoring practices and corrective measures are adopted. It has been reported that periodic monitoring of the skin temperature distributions of process plant tubes at regular intervals is essential to ensure optimum yield, longer service lives of the tubes and safe functioning of the plant [155]. Ge et al. used IRT for performance monitoring of direct air-cooled power generating units [156]. They inspected the temperature distributions of the air-cooled condensers using IRT and studied the effects of ambient air temperature, natural air flow and surface defects on the performance of the units. Studies indicate that IRT can be used for condition monitoring of wind turbine structures to prevent premature failure of the turbine blades during operation [157–162]. Li et al. used IRT to study the effects of the Reynolds number, width and height of the fin and nozzle tip to fin tip distance on the thermal performance of various types of heat sinks with confined impinging jet [163]. Studies indicated that IRT is useful for condition monitoring of paper finishing machines [164], online temperature measurement in hot rolling of aluminum [165], temperature measurement in injection molding and blow molding of plastics [166] and condition monitoring of refinery equipment [167]. Leemans et al. used IRT for condition monitoring of rotating machines [168]. They developed an auto-recursive model for determination of accurate temperature and found that even temperature drifts

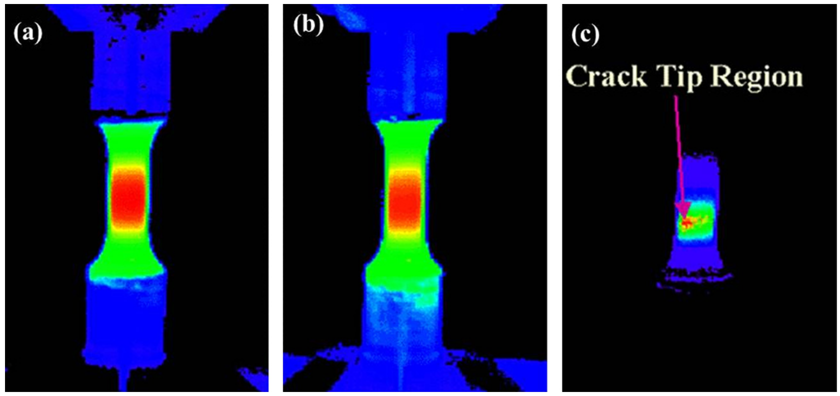

Fig. 8. Infrared thermal image of fatigue testing of a reactor pressure vessel steel (SAA533B1I2) specimen [153]. (a) After 280,000 cycles. (b) After 285,000 cycles. (c) Subtracted image showing the position of fatigue crack tip.

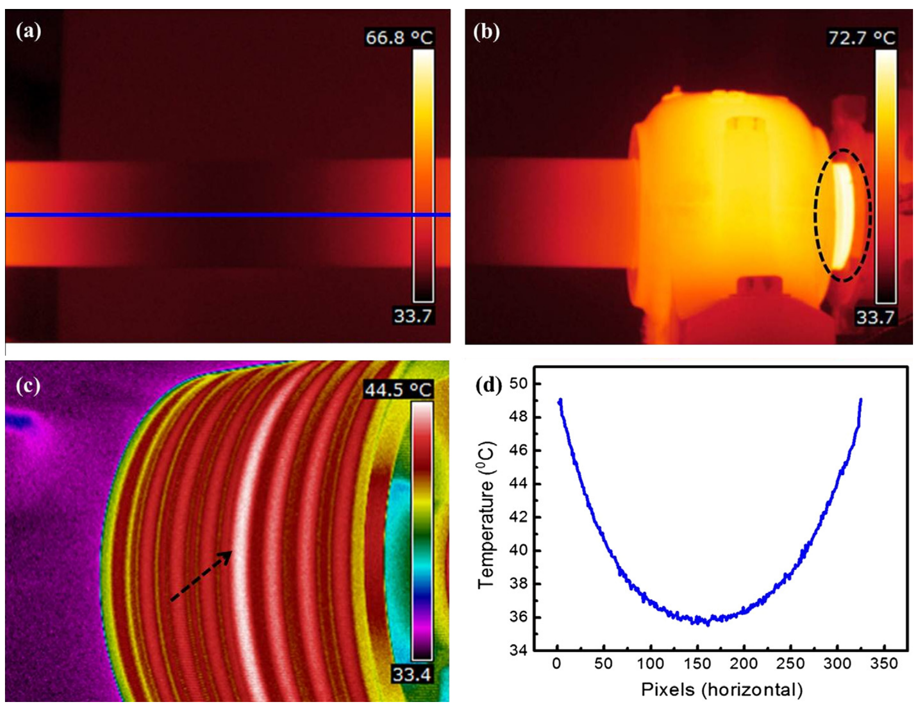

Fig. 9. (a) Infrared thermal image of the shaft of an exhaust system blower under normal operating condition. (b) Thermal image of the impeller end of the exhaust system blower. The abnormal temperature rise (encircled region) was attributed to improper gland packing. (c) Abnormal temperature distribution in the shaft belt due to over-tightening. (d) Temperature profile along the length of the shaft (as indicated by the blue line in figure (a)). It can be seen from the graph that under normal operating condition of the shaft, a symmetric temperature profile was obtained. Any departure from such symmetric profiles may indicate probable misalignment of the shaft. Studies identified the faults beforehand and suitable maintenance work was carried out to avoid any unwarranted failure of the blower systems. (For interpretation of the references to color in this figure legend, the reader is referred to the web version of this article.)

less than 1 °C could be detected using this model, which helped to predict potential modes of failure beforehand. Studies indicate that approximately half of the machine failures occur due to faulty bearings globally [21,22]. Kim et al. used IRT for detecting faults in rotating deep-grooved ball bearings [169]. Mazioud et al. reported that IRT can be used for the detection of rolling bearing degradation (like spalling) and the rise in temperature could be correlated with the level of vibration [170]. Gaberson highlighted that, IRT can be used for investigating energy loss due to misalignment of rotating machines and reported that misalignment can cause up to 2% energy loss, which in turn can increase the temperature of the component significantly [171]. Bagavathiappan et al. used IRT for condition monitoring of the bearings, shaft and motor of exhaust system blowers used in ventilation system of a nuclear power plant [21]. Abnormal temperature rise at the bearing and shaft of the impeller end of the blower was observed, which was attributed to excess heating due to defective gland packing. Additionally, they found that the abnormal temperature distribution in one of the belts of the pulley drive system was due to over-tightening. Fig. 9a–c shows the typical thermal images of the shaft, impeller end and shaft belt of the exhaust system blower respectively. The horizontal temperature profile of the properly aligned shaft is also shown in Fig. 9d. The hotspot is due to defective gland packing at the impeller end (encircled region in Fig. 9b) and the abnormal temperature distribution of the shaft belt due to over-tightening (indicated by an arrow in Fig. 9c) can be clearly seen from the respective thermal images. IRT based condition monitoring of mechanical equipment ensures proper and healthy operation of plants, reduces down-time and maintenance cost and increases the plant efficiency.

5.5. Corrosion monitoring

Corrosion causes huge economic losses across various industrial sectors. A recent study indicates that in United States of America (USA) the total annual direct cost related to corrosion is almost $276 billion [172]. As corrosion is accompanied with loss of materials, it causes surface temperature variations and hence, IRT is an excellent tool for monitoring the surface temperature changes associated with corrosion damages. Grinzato and Vavilov used transient IRT techniques for characterization of hidden corrosion defects [173]. They developed a 3D heat transfer model for corrosion damages and proposed a simple surface temperature time derivative based algorithm for detection of corrosion induced thickness variation. Grinzato et al. applied a simple 1D thermal model to thick cylindrical and spherical components for corrosion detection where heating protocol was optimized for improving the SNR [174]. They reported that corroded areas can be characterized by maximum thermal contrast and appearance time of the maximum contrast value. Marinetti and Vavilov used IRT for detection and characterization of hidden corrosion defects in thick metallic components [175]. Han and Park used IRT for detection of corrosion in steel components coated with organic material where it was observed that temperature difference was highest for ruptured blister kind of defects [176]. Similar studies were also performed by Jonsson et al. [177] and Schonberger et al. [178]. IRT has also been used for detection of corrosion defects in aircraft aluminum panels [179]. Liu et al. used pulsed IRT techniques for quantification of pitting corrosion defects in iron pipes [180]. Phase congruency measurement and principal component analysis were performed and it was observed that the second principal component shows a linear relationship with material loss. Studies show that the acceptable level of accuracy in IRT based techniques is only achievable when there is at least 20% wall thickness loss due to corrosion [181]. Hermanson and Sandor illustrated the applicability of forced diffusion thermography and frame subtraction based image processing algorithm for corrosion fatigue modeling [182]. Chung et al. used IRT for measuring corrosion in reinforced bars where it was observed that the rate of temperature rise increases with the extent of corrosion [183]. Shen and Li reported that IRT is a powerful tool for detecting corrosion pits and wall loss defects in high temperature pipelines which are most commonly used in petrochemical plants and power stations [184]. Their studies indicated that IRT could easily detect corrosion defects bigger than 10 mm in diameter and 40% wall thickness in depth. Fig. 10 shows the infrared thermal images of the corroded areas in an aluminum metallic plate [185]. It can be seen that the corroded regions can be easily localized from the phase image shown in Fig. 10b. Corrosion induced defects reduce the service life of components and IRT based non-contact condition monitoring provides an estimate of material loss due to corrosion and thereby helps in remaining life assessment of the components.

5.6. Weld monitoring

Welding is one of the most widely used joining methods for metallic as well as non-metallic materials. The weld joints are the origins of structural weakness in most of the cases and hence, weld joints must be routinely monitored to ensure structural integrity of the fabricated products. Farley et al. indicated that the probability of weld failure is directly proportional to the probability of NDT missing the flaw [186]. Safety of the welded joints can be ensured by total quality control, i.e., online monitoring of fabrication process and NDT of the finished welded joints. IRT can be regarded as a powerful tool for both of these processes. Meola et al. used IRT for post weld condition monitoring of laser welded SS and adhesively bonded aluminum joints and concluded that the technique provides valuable information about the structural integrity of the welded joints [24]. Pulsed and lock-in thermography techniques were employed for inspection of the welded joints and it was observed that extension of the heat affected zone could be determined from the acquired phase images. It was also verified, using IRT, that heat affected zone becomes narrower as the welding speed increases. IRT has been widely used for online weld penetration monitoring [187–191], control of welding processes [192–195], material deposition control [196], weld system control [197], quality assurance of laser welding [198], online quality monitoring of abrasive water jet (AWJ) cutting process [199], monitoring of resistance spot welding [200] and friction stir welding (FSW) processes [201]. Venkatraman et al. used IRT for online detection of incomplete penetration and penetration depth estimation during TIG welding and reported that surface temperature profile shows linear correlation with penetration depth [202]. Sreedhar et al. used IRT for online weld quality monitoring and automatic detection of defects [27]. Their studies indicate that offset positioned IRT based online monitoring of TIG welding is capable of detecting porosities. They further reported that the spatial and time dependence of temperature near the weld pool could provide valuable information regarding possible defects in the welded regions. IRT has also been used for online monitoring and quality control of no-metallic (like polymer, wood, etc.) welding processes. Kafieh et al. used IRT for automatic detection of defects in polyethylene pipes [25]. Infrared thermal video sequences were acquired during the post-weld cooling phase and a clustering algorithm based image processing was performed to characterize the defects. Speka et al. used IRT for parameter optimizations during transmission mode laser welding of amorphous polymer specimens [203]. Ganne-Chedeville et al. used IRT for studying the wood welding parameters where the maximum and average peak temperature, temperature distribution and rate of temperature increase were measured near the welded regions and the effects of these parameters on the weld integrity were studied in detail [204]. Nandhitha et al. discussed various feature extracting algorithms for processing of the infrared thermal images acquired during online weld monitoring and reported that Euclidean distance based color image segmentation algorithm is best suited for the purpose [205]. Lahiri et al. used IRT for detection and quantification of weld defects in friction stir welded aluminum joints and tungsten inert gas (TIG) welded SS joints [26]. The defect depths were estimated using lock-in thermography technique. The results were confirmed using digital X-ray radiography technique. Fig. 11a–d shows the photographs and lock-in images of TIG welded SS joints with lack of fusion and tungsten inclusion defects respectively. It must be noted that all the defects could be clearly identified from the thermography images. Based on the above case studies it can be concluded that IRT is an excellent technique for defect detection in welded joints and compared to other non-contact NDT techniques, lock-in thermography is preferable because it provides information about defect depth also. IRT is a matured and widely accepted condition monitoring tool for inspection of weld joints and online monitoring welding processes and provides sufficient information for quality assurance of weld joints which will in turn ensure the structural integrity of weld joints thereby reducing the risk of sudden failures.

5.7. Application of IRT in nuclear industries

IRT has been widely applied for condition monitoring of various components of nuclear industries. IRT can be reported to be successfully used for condition monitoring of the annulus fan bearings

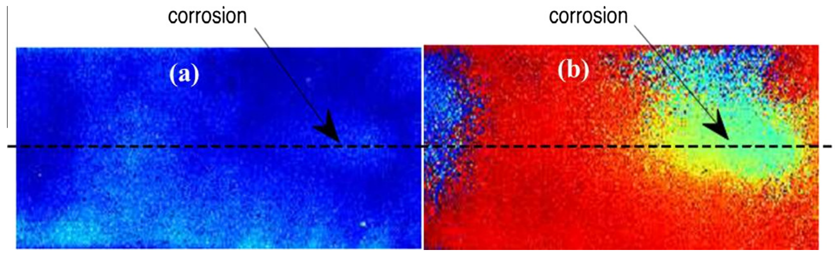

Fig. 10. Infrared thermography is a potential tool for corrosion detection [185]. Artificial defects were fabricated on an aluminum specimen and a modulated heat source was used for heating the specimens. The infrared images were acquired at regular interval. (a) Amplitude image. (b) Phase image. The corroded regions could be easily seen in the phase image.

and motor faults located on top of the radioactive liquid waste tank, cooling water pump, slurry pump, exhaust fans and electrical components like panels, circuit breakers, relays, etc. at the Savannah riverside nuclear installations in USA [206]. Lewak has described the various applications of IRT in several commercial nuclear installations across USA in detail [207]. He has illustrated the applications of IRT with numerous detailed case studies for defect detection in fiber–glass reinforced plastic materials used in the critical components of negative pressure reactor safety systems and fiber reinforced rubber materials which are used as sealant in earlier generation Canadian deuterium uranium (CANDU) reactors. Rodriguez and Raj has used IRT for condition monitoring of various components of a nuclear power plant like main transformer, switchyard, concrete walls of turbine building, etc. [208]. Lee and Kim used IRT for early detection and condition monitoring of heavy water leakage out of the fuel channel closure-plugs of a heavy water reactor during operation [209]. They observed that using IRT, the location of the leakages could be identified and the leak status could be monitored in real-time during the reactor operation and concluded that IRT can be considered as a powerful tool for condition monitoring of operational nuclear reactors. Kim et al. used ultrasound pulsed phase thermography for real time crack detection in the austenitic STS304 specimens, which are used for piping in reactor coolant systems [210]. Madurga et al. applied IRT for real-time monitoring and controlling of the cooling process of lead shields during the fabrication stages of the nuclear fuel transport containers [211]. IRT has been used for condition monitoring of a heavy water plant which employs ammonia-hydrogen isotopic chemical exchange process [212]. The ammonia cracker tubes should be operated at their designed optimum temperature and must not exceed the maximum limit of 993 K. High temperature operation of these tubes may cause loss of ductility, intergranular cracking or creep damage which may lead to failure of the tubes, whereas, low temperature operation will lead to incomplete cracking of ammonia resulting in lower yield. IRT was used for estimating the surface temperature of the cracker tubes and to visualize the thermal gradients across the tubes as a function of elevation. The flames in the background and restricted optical access presented major experimental difficulties for IRT measurements. The thermal images were acquired during night time and through a small circular opening available at various elevation stages.

Itami et al. developed multiplexing thermography technique for the divertor of the International Thermonuclear Experimental Reactor (ITER) for measuring the effects of the edge localized mode (ELM) heat fluxes, which may cause severe erosion of the divertor [34]. The authors reported that, survivability issues under plasma discharge and redeposition related surface problems may present major experimental challenges. Courtois et al. used lock-in IRT for health monitoring of the controlled plasma facing components of the Tore-Supra (TS) toroidal pump during maintenance shutdown [213]. This technique was successfully tested under laboratory conditions and the authors concluded that IRT can be considered as a qualitative method for detecting serious flaws on the refractory armour tile and heat sink interface. The studies also indicate that a few flawed tiles could be clearly identified in a recent in situ campaign using the lock-in IRT method. A transient IRT technique called station acquisition et traitement infrarouge (SATIR) was developed by French atomic energy commission (CEA) for condition monitoring and quality control of the manufactured plasma facing components for the fusion reactor. Durocher et al. used SATIR methodology for inspection of the ITER vertical components manufactured by the European industries [214]. Gauthier et al. used IRT for the study of ELM heat flux interactions in an ITER-like wide angle infrared and visible diagnostic using reflecting optics [215]. The acquired infrared thermal images showed that the major plasma wall interactions were located on the divertor, but significant amount of interactions were also present on the upper and outer limiters. Fig. 12a and b shows a typical photograph of internal components of the joint European torus (JET) vessel and the infrared image of the JET vessel during edge localized mode (ELM) discharge respectively [215]. The infrared image shows the temperature difference between two consecutive frames, one before the ELM discharge and one after the discharge. Online monitoring of various safety–critical systems of nuclear power plants using IRT will ensure structural integrity of the systems and in many cases major failures and damages could be avoided.

5.8. IRT based condition monitoring in aerospace industries

IRT is one of the most commonly used tools for condition monitoring in aerospace industries. Several types of light weight composite structures (like carbon and glass fiber reinforced polymers, honeycomb structures, sandwich panels, etc.) are routinely used for fabrication of aerospace components. These components are prone to defects like delaminations, de-bonds, foreign inclusions, porosity, water ingress, node failure and core crushing. Periodical monitoring of the fabricated components are required for ensuring structural integrity. IRT is a widely accepted condition monitoring tool in aerospace industry primarily because inspection can be carried out on large areas without dismantling aircraft components. As the process is non-contact in nature inspection time is considerably lower than other condition monitoring techniques. In general, moisture corrodes the honeycomb structures and at the same time adhesive strength is also reduced. Hence detection of water ingress is composite structures is of prime importance. Saarimaki and Ylinen used IRT based techniques for detection of water penetration in composite materials [216]. The whole structure is cooled below freezing point of water and subsequently warmed up to room temperature. Phase transition energy (required for melting of water) was detected using IRT and the location of water penetration could be identified from the thermograms. In general inspections of the composite parts are carried out after fabrication or in situ (after a

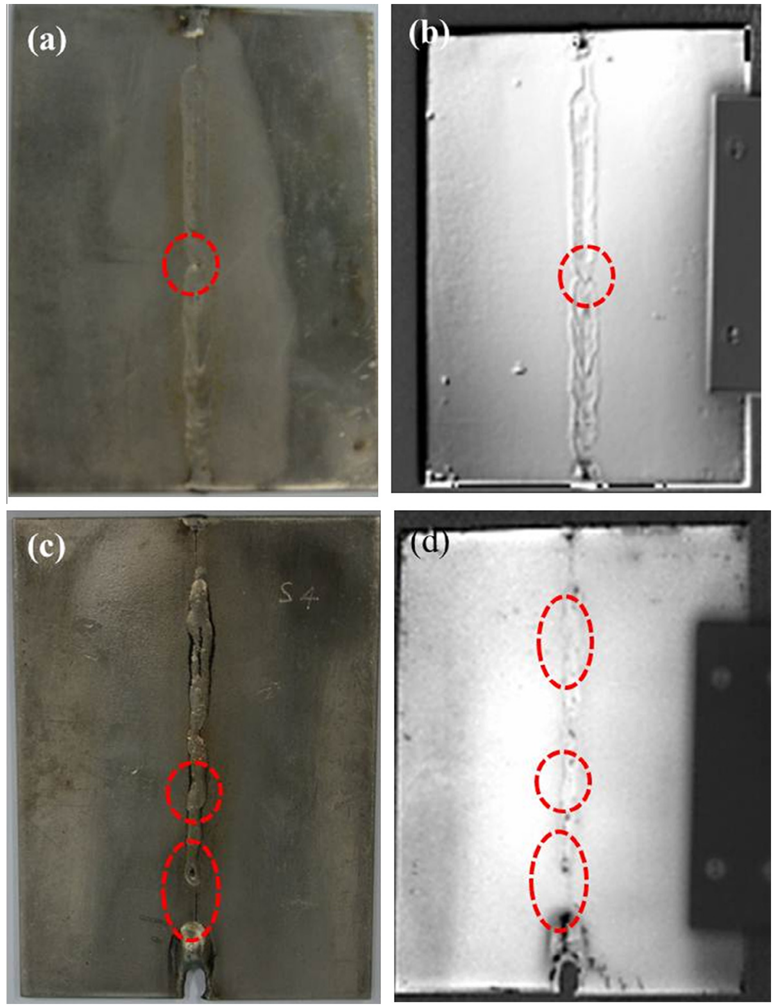

Fig. 11. (a) Photograph of a tungsten inert gas (TIG) welded stainless steel (SS) joint with lack of fusion (LOF) defect. (b) Lock-in thermography image (excitation frequency: 0.1436 Hz) of the LOF specimen. (c) Photograph of a TIG welded SS joint with tungsten inclusion (TI) defect. (d) Lock-in thermography image (excitation frequency: 0.1266 Hz) of the TI specimen. It is evident that all the defects (encircled in red) could be easily identified from the infrared thermal images. The advantage of lock-in thermography over other techniques is that it additionally provides depth information also. (For interpretation of the references to color in this figure legend, the reader is referred to the web version of this article.)

few hours of landing). For inspection purposes, active thermography techniques are preferable as external heating is required for producing thermal contrast between the defect and defect-free regions. Reflection mode (camera and heat source are on the same side) is in general adopted as most of the components have single side access. Ibarra-Castanedo et al. presented a detailed study on active thermography techniques (pulsed, lock-in, pulsed phase, vibro-thermography) on light weight structural materials like honey-comb panels [77,217]. The studies indicate that though optical excitations resulted in good defect resolution, the results are strongly affected by surface features. Advanced signal processing techniques could reduce the impact of the surface conditions. They reported that defects (diameter to depth ratio of 2 or higher) of depth 2.5 mm could be detected using pulsed phase thermography and thermographic signal reconstruction techniques. Meola et al. used IRT for monitoring the damages (delamination, impact damages, fatigue failure, etc.) in various aerospace materials like composites, hybrid composites, sandwich structures and recommended that IRT must be integrated with the industrial instrumentation for monitoring the entire fabrication process and subsequent quality assurance [218]. Robotic arrangement for automated thermography of large components of fiber reinforced polymers has been developed by aerospace industries [219]. Such automated systems will reduce the inspection time drastically. Menaka et al. used IRT for inspecting variations in glue content and defect detection in adhesively bonded canopy specimens used in fighter aircrafts [36]. The specimens were uniformly heated and the thermal contrast between the regions with normal and reduced glue content were monitored. This study shows that infrared thermal imaging is a highly sensitive technique to detect variation (>20%) in glue content. Burleigh described several diversified applications of IRT in aerospace industries like thermographic nondestructive testing of composite materials and structures, thermal mapping of aerodynamically heated components, thermographic studies of gas plumes ejected from jet and rocket engines, temperature monitoring of electrical de-icers on helicopter rotor blades, detection of cooling system blockages in jet engine turbine blades, etc. [220]. Meola and Carlomagno reviewed several applications of IRT in modeling of aerodynamics [221]. Fig. 13 shows typical infrared thermal images of the cockpit region of an aircraft, where insulation defects can be clearly seen [222].

5.9. Other applications

IRT has been successfully used in postharvest quality control, grain quality monitoring and detection of foreign bodies in food

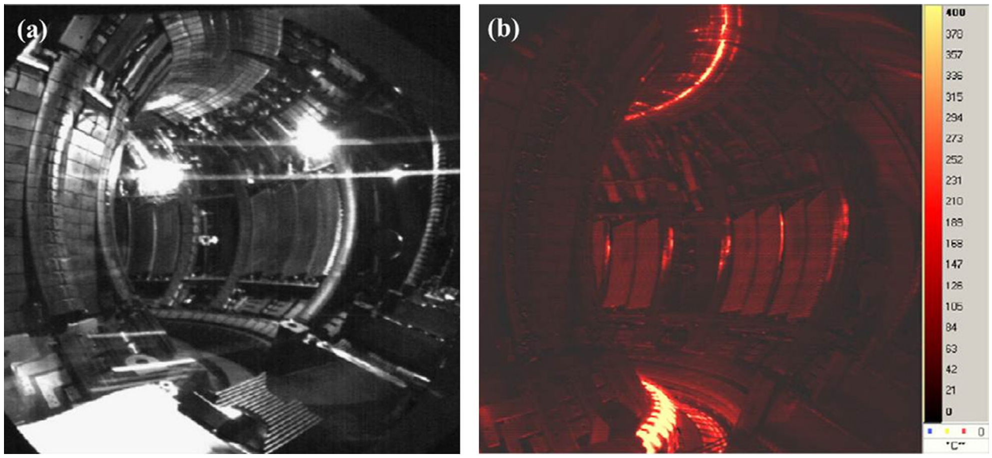

Fig. 12. Infrared thermography can also be used for condition monitoring of nuclear components [215]. (a) A typical photograph of internal components of the joint European torus (JET) vessel used for fusion reactor experiments. (b) Infrared image of the JET vessel during edge localized mode (ELM) discharge. The image shows the temperature difference between two consecutive frames: one before the ELM discharge and one after the discharge.

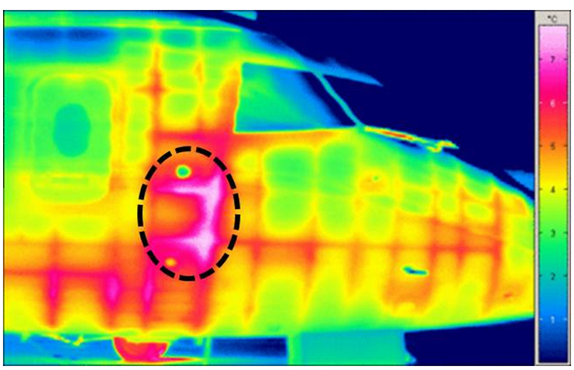

Fig. 13. (a) Infrared thermal image of the cockpit off an aircraft [222]. The insulation failures can be clearly seen from the thermal images.

items [37]. IRT has also been used for several other applications in food industries like surface quality monitoring of apples [223], monitoring surface drying of citrus fruits [224], assessment of pork and raw ham quality, etc. [225]. Song and Shida used IRT for measurement of surface temperature to control the drying condition of Japanese cedar lumber wood to reduce surface checking (small cracks on the surface) [226]. Plescanu et al. used IRT to investigate the structure of flooded wooden floors and found that IRT is useful to study the drying process and localization of the wet areas [227]. IRT has found its application in paper industry also. Kiiskinen et al. used IRT for monitoring paper cockling, moisture formation, thermal non-uniformity and analysis of the paper failure mechanisms [40]. Hojjatie et al. used IRT for quantitative determination of in-plane moisture distribution in paper [41]. The studies reported that lower moisture content areas appeared as hotter regions in the acquired thermal images and there exist a linear correlation between the moisture content and the surface temperature values. IRT has also been applied to marine industry for inspection of electrical and mechanical systems of ships, mobile marine systems, to monitor the quality of sea water surface and to detect any pollution or leakage of hazardous materials [228].

6. Conclusion

Infrared thermography has evolved as an effective condition monitoring tool for real-time temperature monitoring of objects or processes in a non-contact way. It provides pertinent information regarding the health and efficiency of equipment or processes which are very crucial to prevent catastrophic breakdown or emergency shutdown. The applications of modern image processing tools on the acquired infrared thermal images along with artificial intelligence based approaches can further augment the decision making process faster and without human interference. Unlike other condition monitoring methodologies, infrared thermography provides a real-time pseudo color coded image of the object and visual manifestation of defects. Applications of IRT as a condition monitoring technique in civil structures, electrical installations, machineries and equipment, material deformation under various loading conditions, corrosion damages, welding processes, nuclear, aerospace, food, paper, wood and plastic industries are reviewed. This review would also enable non-specialist in industries to adopt this technique for various condition monitoring applications, which would reduce down-time, maintenance cost, risk of accidents and enhance the productivity and growth.

Acknowledgement

Authors thank Dr. B.P.C. Rao for encouragements and support.

Reference

[1] I.B. Utne, T. Brurok, H. Rodseth, A structured approach to improved condition monitoring, Journal of Loss Prevention in the Process Industries 25 (2012) 478–488.
[2] C.R. Farrar, K. Worden, An introduction to structural health monitoring, Philosophical Transactions of Royal Society A 365 (2007) 303–315.
[3] M.C. Eti, S.O.T. Ogaji, S.D. Probert, Reducing the cost of preventive maintenance (PM) through adopting a proactive reliability-focused culture, Applied Energy 83 (2006) 1235–1248.
[4] B.K.N. Rao, Condition monitoring and the integrity of industrial systems, in: A. Davies (Ed.), Handbook of Condition Monitoring: Techniques and Methodologies, Chapman & Hall, London, UK, 1998.
[5] P.A. Bragatto, P. Pittiglio, S. Ansaldi, The management of mechanical integrity inspections at small-sized "Seveso" facilities, Reliability Engineering and System Safety 94 (2009) 412–417.
[6] A. Al-Habaibeh, F. Zorriassatine, N. Gindy, Comprehensive experimental evaluation of a systematic approach for cost effective and rapid design of condition monitoring system using Taguchi's method, Journal of Material Processing Technology 124 (2002) 372–383.
[7] R.A. Epperly, G.E. Heberlein, L.G. Eads, A tool for reliability and safety: predict and prevent equipment failures with thermography, in: IEEE Petroleum and Chemical Industry Conference, Banff, Alta, 1997, pp. 59–68.
[8] E. Grinzato, C. Bressan, S. Marinetti, P.G. Bison, C. Bonacina, Monitoring of the Scrovegni Chapel by IR thermography: Giotto at infrared, Infrared Physics & Technology 43 (2002) 165–169.
[9] M.R. Clark, D.M. McCann, M.C. Forde, Application of infrared thermography to the non-destructive testing of concrete and masonry bridges, NDT&E International 36 (2003) 265–275.

[10] C. Meola, Infrared thermography for masonry structure, Infrared Physics & Technology 49 (2007) 228–233.
[11] M.S. Jadin, S. Taib, Recent progress in diagnosing the reliability of electrical equipment by using infrared thermography, Infrared Physics & Technology 55 (2012) 236–245.
[12] Y. Cao, X. Gu, Q. Jin, Infrared technology in the fault diagnosis of substation equipment, in: China International Conference on Electricity Distribution, Guangzhou, China, 2008.
[13] F. Lizak, M. Kolcun, Improving reliability and decreasing losses of electrical system with infrared thermography, Acta Electrotechnica et Informatica 8 (2008) 60–63.
[14] C. Badulescu, M. Grediac, H. Haddadi, J.-D. Mathias, X. Balandraud, H.-S. Tran, Applying the grid method and infrared thermography to investigate plastic deformation in aluminium multicrystal, Mechanics of Materials 43 (2011) 36–53.
[15] B. Venkataraman, B. Raj, C.K. Mukhopadhyay, T. Jayakumar, Correlation of infrared thermographic patterns and acoustic emission signals with tensile deformation and fracture processes, in: D.O. Thompson, D.E. Chiment (Eds.), Review of Progress in Quantitative Nondestructive, Evaluation, 2001, pp. 1443–1450.
[16] J. Kumar, S. Baby, V. Kumar, Thermographic studies on IMI-834 titanium alloy during tensile loading, Material Science and Engineering A 496 (2008) 303–307.
[17] H. Ait-Amokhtar, C. Fressengeas, S. Boudrahem, The dynamics of Portevin–Le Chatelier bands in an Al–Mg alloy from infrared thermography, Material Science and Engineering A 488 (2008) 540–546.
[18] M.P. Luong, Fatigue limit evaluation of metals using an infrared thermographic technique, Mechanics of Materials 28 (1998) 155–163.
[19] M.L. Pastor, X. Balandraud, M. Grediac, J.L. Robert, Applying infrared thermography to study the heating of 2024-T3 aluminium specimens under fatigue loading, Infrared Physics & Technology 51 (2008) 505–515.
[20] H. Wang, L. Jiang, P.K. Liaw, C.R. Brooks, D.L. Klastrom, Infrared temperature mapping of ULTIMET alloy during high-cycle fatigue, Metallurgical and Materials Transaction A 31A (2000) 1307–1310.
[21] S. Bagavathiappan, T. Saravanan, N.P. George, J. Philip, T. Jayakumar, B. Raj, Condition monitoring of exhaust system blowers using infrared thermography, Insight 50 (2008) 512–515.
[22] D. Kim, H. Yun, S. Yang, W. Kim, D. Hong, Fault diagnosis of ball bearing within rotational machines using the infrared thermography method, Journal of Korean Society of Nondestructive Testing 30 (2010) 570–575.
[23] J. Seo, H. Yoon, H. Ha, D. Hong, W. Kim, Infrared thermographic diagnosis mechanism for fault detection of ball bearing under dynamic loading conditions, Advanced Materials Research 295–297 (2011) 1544–1547.
[24] C. Meola, G.M. Carlomagno, A. Squillace, G. Giorleo, The use of infrared thermography for nondestructive evaluation of joints, Infrared Physics & Technology 46 (2004) 93–99.
[25] R. Kafieh, T. Lotfi, R. Amirfattahi, Automatic detection of defects on polyethylene pipe welding using thermal infrared imaging, Infrared Physics & Technology 54 (2011) 317–325.
[26] B.B. Lahiri, S. Bagavathiappan, T. Saravanan, K.V. Rajkumar, A. Kumar, J. Philip, T. Jayakumar, Defect detection in weld joints by infrared thermography, in: International Conference on NDE in Steel and allied Industries, NDESAI, 2011, Jamshedpur, India, 2011, pp. 191–197.
[27] U. Sreedhar, C.V. Krishnamurthy, K. Balasubramanian, V.D. Raghupathy, S. Ravisankar, Automatic defect identification using thermal image analysis for online weld quality monitoring, Journal of Materials Processing Technology 212 (2012) 1557–1566.
[28] M. Vellvehi, X. Perpina, G.L. Lauro, F. Perillo, X. Jorda, Irradiance-based emissivity correction in infrared thermography for electronic applications, Review of Scientific Instruments 82 (2011) 114901.
[29] S. Huth, O. Breitenstein, A. Huber, D. Dantz, U. Lambert, F. Altmann, Lock-in IR thermography – a novel tool for material and device characterization, Solid State Phenomena 82–84 (2002) 741–746.
[30] R. Lehtiniemi, C.-M. Fager, A.-M. Hynninen, T. Aapro, P. Tiilikka, V. Kyyhkynen, J. Rantala, Applications of infrared thermography in electronics research, in: 5th International Conference on Quantitative Infrared Thermography, Reims, France, 2000.
[31] E.J. Johnson, P.V. Hyer, P.W. Culotta, I.O. Clark, Evaluation of infrared thermography as a diagnostic tool in CVD applications, Journal of Crystal Growth 187 (1998) 463–473.
[32] R.D. Lucier, J.C. Bognet, Thermography in commercial nuclear power stations, applications, limitations, and realities, in: G.B. McIntosh (Ed.), SPIE, Thermosense XI: International Conference on Thermal Infrared Sensing for Diagnostics and Control, Orlando, FL, 1989, pp. 56.
[33] J.J.E. Black, Thermal baseline factors in nuclear power plants, in: G.B. McIntosh (Ed.), SPIE, Thermosense XI: International Conference on Thermal Infrared Sensing for Diagnostics and Control, Orlando, FL, 1989, pp. 62.
[34] K. Itami, T. Sugie, G. Vayakis, C. Walker, Multiplexing thermography for international thermonuclear experimental reactor divertor targets, Review of Scientific Instruments 75 (2004) 4124–4128.
[35] L.D. Favro, T. Ahmed, X. Han, L. Wang, S.M. Shepard, Thermal wave imaging of aircraft structures, Review of Progress in Quantitative Non-Destructive Evaluation 14 (1995) 461–466.
[36] M. Menaka, S. Bagavathiappan, B. Venkatraman, T. Jayakumar, B. Raj, Characterisation of adhesively bonded laminates using radiography and infrared thermal imaging techniques, Insight 48 (2006) 606–612.
[37] A.A. Gowen, B.K. Tiwari, P.J. Cullen, K. McDonnell, C.P. O'Donnell, Applications of thermal imaging in food quality and safety assessment, Trends in Food Science & Technology 21 (2010) 190–200.
[38] A. Wyckhuyse, X. Maldague, Study of wood inspection by infrared thermography, part I: wood pole inspection by infrared thermography, Research in Nondestructive Evaluation 13 (2001) 1–12.
[39] J.P.d.B. Filho, J.R. Henriquez, Infrared thermography applied for high-level current density identification over planar microwave circuit sectors, Infrared Physics & Technology 53 (2010) 84–88.
[40] H.T. Kiiskinen, H.K. Kukkonen, P.I. Pakarinen, A.J. Laine, Infrared thermography examination of paper structure, TAPPI Journal 80 (1997) 159–162.
[41] B. Hojjatie, J. Abedi, D.W. Coffin, Quantitative determination of in-plane moisture distribution in paper by infrared thermography, TAPPI Journal 84 (2001) 71–81.
[42] G.C. Holst, Common Sense Approach to Thermal Imaging, JCD Publishing and SPIE – The International Society for Optical Engineering, Winter Park, FL and Bellingham, WA, 2000.
[43] C.W. Reeves, Thermography Monitoring Handbook, Coxmoor Publishing Company, 1999.
[44] X.P.V. Maldague, Infrared methodology and technology, in: W.J. McGonnagle (Ed.), Nondestructive Testing Monographs and Tracts, Gordon and Breach Science Publishers, 1994.
[45] C. Meola, Infrared Thermography Recent Advances and Future Trends, Bentham eBooks, 2012.
[46] C. Meola, Origin and theory of infrared thermography, in: C. Meola (Ed.), Infrared Thermography Recent Advances and Future Trends, Bentham eBooks, 2012, pp. 3–28.
[47] H. Qi, N.A. Diakides, Infrared Thermal Imaging, <http://www.aicip.ece.utk.edu/publication/06thermography.pdf>.
[48] Z.M. Zhang, B.K. Tsai, G. Machin, Radiometric Temperature Measurements, Academic Press, Oxford, 2010.
[49] D.P. Jones, Biomedical Sensors, Momentum Press, New York, 2010.
[50] R. Rinaldi, Infrared devices: short history and new trends, in: C. Meola (Ed.), Infrared Thermography Recent Advances and Future Trends, Bentham eBooks, 2012, pp. 29–59.
[51] B. Venkataraman, B. Raj, Performance parameters for thermal imaging systems, Insight 45 (2003) 531–535.
[52] B.B. Lahiri, S. Bagavathiappan, T. Jayakumar, J. Philip, Medical applications of infrared thermography: a review, Infrared Physics & Technology 55 (2012) 221–235.
[53] E.F.J. Ring, The historical development of temperature measurement in medicine, Infrared Physics & Technology 49 (2007) 297–301.
[54] S. Bagavathiappan, J. Philip, T. Jayakumar, B. Raj, P.N.S. Rao, M. Varalakshmi, V. Mohan, Correlation between plantar foot temperature and diabetic neuropathy: a case study by using an infrared thermal imaging technique, Journal of Diabetes Science and Technology 4 (2010) 1386–1392.
[55] X. Maldague, Theory and Practice of Infrared Technology for Nondestructive Testing, first ed., John Wiley and Sons, New York, 2001.
[56] C. Maierhofer, A. Brink, M. Rollig, H. Wiggenhauser, Transient thermography for structural investigation of concrete and composites in the near surface region, Infrared Physics & Technology 43 (2002) 271–278.
[57] B.B. Lahiri, S. Bagavathiappan, P.R. Reshmi, J. Philip, T. Jayakumar, B. Raj, Quantification of defects in composites and rubber materials using active thermography, Infrared Physics & Technology 55 (2012) 191–199.
[58] R. Montanini, Quantitative determination of subsurface defects in a reference specimen made of plexiglas by means of lock-in and pulsed phase infrared thermography, Infrared Physics & Technology 53 (2010) 363–371.
[59] T. Sakagami, S. Kubo, Applications of pulse heating thermography and lock-in thermography to quantitative nondestructive evaluations, Infrared Physics & Technology 43 (2002) 211–218.
[60] C. Meola, Non-destructive control of industrial materials by means of lock-in thermography, Measurement Science & Technology 13 (2002) 1583–1590.
[61] S. Gasperic, B. Sprajcar, R. Bernard, R. Glavic, The analysis of thermographic reports with emphasis on emissivity coefficient determination of bare conductors and joints, in: Proceedings of the 21st International Conference on Electricity, Distribution, Vienna, 2007.
[62] L.D. Santos, E.C. Bortoni, L.E. Souza, G.S. Bastos, M.A.C. Craveiro, Infrared thermography applied for outdoor power substations, in: V.P. Vavilov, D.D. Burleigh (Eds.), Proceedings of the SPIE 6939: Thermosense XXX, Orlando, FL, 2008, pp. 69390R.
[63] http://www.monarchserver.com/TableofEmissivity.pdf (Table of Total Emissivity).
[64] B. Venkatraman, C.K. Mukhophadyay, B. Raj, Prediction of tensile failure of 316 stainless steel using infrared thermography, Experimental Techniques (2004) 35–38.
[65] N.P. Avdelidis, A. Moropoulou, Emissivity considerations in building thermography, Energy and Buildings 35 (2003) 663–667.
[66] D.T. Dumpert, Infrared techniques for printed circuit board (PCB) evaluation, in: X.P.V. Maldague (Ed.), Infrared Methodology and Technology, Gordon and Breach Science Publishers, Great Britain, 1994, pp. 253–264.
[67] E. Barreira, V.P.d. Freitas, Evaluation of building materials using infrared thermography, Construction and Building Materials 21 (2007) 218–224.
[68] D.J. Titman, Applications of thermography in non-destructive testing of structures, NDT&E International 34 (2001) 149–154.

[69] Y.C. Chieh, L. Yao, Automatic diagnostic system of electrical equipment using infrared thermography, in: Proceedings of International Conference on Soft Computing and Pattern Recognition, 2009, pp. 155–160.
[70] T.M. Lindquist, L. Bertling, R. Eriksson, Estimation of disconnector contact condition for modelling the effect of maintenance and aging, in: Proceedings of the Russia Power Tech., 2005.
[71] Maintenance Testing Specifications for Electric Power Distribution Equipment and Systems, NETA (MTS-1997), International Electrical Testing Association, Inc., Morrison CO, 1997.
[72] ASTM E 1934-99a (Reapproved 2010): Standard Guide for Examining Electrical and Mechanical Equipment with Infrared Thermography.
[73] NFPA 70B: Recommended Practice for Electrical Equipment Maintenance, National Fire Protection Association, Quincy, Massachusetts, 2006.
[74] Infrared Thermal Imaging Survey Procedure for Electrical Equipment, MIL-STD-2194, Naval Sea Systems, 1988.
[75] Service/Repair Guidance for Allen-Bradley Company Bulletin 2100/2400 Motor Control Center Units Based on Field Temperature Analysis, Allen-Bradley Company, Dev. Tech. Data 2.2, May, 1993.
[76] Standard for Infrared Inspection of Electrical Systems & Rotating Equipment, Infraspection Institute, Burlington, NJ, 2008.
[77] C. Ibarra-Castanedo, E. Grinzato, S. Marinetti, P. Bison, M. Genest, M. Grenier, J.-M. Piau, A. Bendada, X. Maldague, Recent progresses in the inspection of aerospace components by infrared thermography, in: 17th World Conference on Nondestructive Testing, Shanghai, China, 2008.
[78] M. Fidali, An idea of continuous thermographic monitoring of machinery, in: 9th International Conference on Quantitative Infrared Thermography, Krakow, Poland, 2008.
[79] A.T.P. So, W.L. Chan, C.T. Tse, K.K. lee, Fuzzy logic based automatic diagnosis of power apparatus by infrared imaging, in: 2nd International Forum on Applications of Neural Network to Power Systems, 1993, pp. 187–192.
[80] L. Baoshu, Z. Xiaohui, Z. Shutao, N. Wendong, HV power equipment diagnosis based on infrared imaging analyzing, in: Proceedings of the International Conference on the Power System Technology, Chongqing, China, 2006.
[81] N.T. Moja, A.J. Willis, Classification of thermally condition-monitored components using statistical and neural network techniques, in: A.G. Tescher (Ed.), Proceedings of SPIE 3164: Applications of Digital Image Processing XX, San Diego, CA, USA, 1997, pp. 573–581.
[82] J. Shi, J. Malik, Normalized cuts and image segmentation, IEEE Transactions on Pattern Analysis and Machine Intelligence 22 (2000) 888–905.
[83] S. Sahli, S. Fissette, X. Maldague, Infrared image processing for online quality control in laser welding, in: 10th International Conference on Quantitative InfraRed Thermography, Quebec, Canada, 2010.
[84] R.C. Gonzalez, P. Wintz, Digital Image Processing, 2 ed., Addison-Wesley, Reading, Massachusetts, 1987.
[85] T.Z. Tan, C. Queck, G.S. Ng, K. Razvi, Ovarian cancer diagnosis with complementary learning fuzzy neural network, Artificial Intelligence in Medicine 43 (2008) 207–222.
[86] F. Just-Agosto, D. Serrano, B. Shafiq, A. Cecchini, Neural network based nondestructive evaluation of sandwich composites, Composites Part B 39 (2008) 217–225.
[87] S. Vallerand, X. Maldague, Defect characterization in pulsed thermography: a statistical method compared with Kohonen and Perceptron neural networks, NDT&E International 33 (2000) 307–315.
[88] O. Buyukozturk, Imaging of concrete structures, NDT&E International 31 (1998) 233–243.
[89] E. Grinzato, State of the art and perspective of infrared thermography applied to building science, in: C. Meola (Ed.), Infrared Thermography Recent Advances and Future Trends, Bentham eBooks, 2012, pp. 200–229.
[90] S.A. Ljungberg, Infrared techniques in buildings and structures: operation and maintenance, in: X.P.V. Maldague (Ed.), Infrared Methodology and Technology, Gordon and Breach Science Publishers, Great Britain, 1994, pp. 211–252.
[91] S. Datcu, L. Ibos, Y. Candau, S. Mattei, Improvement of building wall surface temperature measurements by infrared thermography, Infrared Physics & Technology 46 (2005) 451–467.
[92] C. Maierhofer, R. Arndt, M. Rollig, Influence of concrete properties on the detection of voids with impulse-thermography, Infrared Physics & Technology 49 (2007) 213–217.
[93] C. Maierhofer, M. Roellig, Active thermography for the characterization of surfaces and interfaces of historic masonry structures, in: Non-Destructive Testing in Civil Engineering, Nantes, France, 2009.
[94] A. Poblete, M.A. Pascual, Thermographic measurement of the effect of humidity in mortar porosity, Infrared Physics & Technology 49 (2007) 224–227.
[95] M. Azenha, R. Faria, H. Figueiras, Thermography as a technique for monitoring early age temperatures of hardening concrete, Construction and Building Materials 25 (2011) 4232–4240.
[96] R.W. Arndt, Square pulse thermography in frequency domain as adaptation of pulsed phase thermography for qualitative and quantitative applications in cultural heritage and civil engineering, Infrared Physics & Technology 53 (2010) 246–253.
[97] E. Grinzato, P.G. Bison, S. Marinetti, Monitoring of ancient buildings by the thermal method, Journal of Cultural Heritage 3 (2002) 21–29.
[98] N.P. Avdelidis, A. Moropoulou, Applications of infrared thermography for the investigation of historic structures, Journal of Cultural Heritage 5 (2004) 119–127.
[99] A. Tavukcuoglu, A. Duzgunes, E.N. Caner-Saltık, S. Demirci, Use of IR thermography for the assessment of surface-water drainage problems in a historical building, Agzikarahan (Aksaray), Turkey, NDT&E International 38 (2005) 402–410.
[100] M.P. Luong, Introducing infrared thermography in soil dynamics, Infrared Physics & Technology 49 (2007) 306–311.
[101] R. Sugiura, N. Noguchi, K. Ishii, Correction of low-altitude thermal images applied to estimating soil water status, Biosystems Engineering 96 (2007) 301–313.
[102] V. Vavilov, V. Demin, Infrared thermographic inspection of operating smokestacks, Infrared Physics & Technology 43 (2002) 229–232.
[103] J.C. Candore, J.L. Bodnar, A. Szeflinski, L. Ibos, S. Datcu, Y. Candau, S. Mattei, J.-C. Frichet, Helps with the thermal diagnosis of the building: detection of defects of insulation by stimulated infra-red thermography, in: 9th International Conference on Quantitative Infrared Thermography, Krakow, Poland, 2008.
[104] RESNET. <http://www.resnet.us/professional/standards>.
[105] C.A. Balaras, A.A. Argiriou, Infrared thermography for building diagnostics, Energy and Buildings 34 (2002) 171–183.
[106] R.B.C. Sales, F.A. Sales, S.G. Tavares, R.M.d. Andrade, M.T.P. Aguilar, Thermal analysis of structural masonry in concrete block containing expanded polystyrene (EPS) using digital infrared thermal image, in: 10th International Conference on Quantitative Infrared Thermography, Quebec, Canada, 2010.
[107] N. Ludwig, Thermographic testing on buildings using a simplified heat transfer model, Materials Evaluation (2003) 599–603.
[108] D.A. Haralambopoulos, G.F. Paparsenos, Assessing the thermal insulation of old buildings – the need for in situ spot measurements of thermal resistance and planar infrared thermography, Energy Conversion and Management 39 (1998) 65–79.
[109] P.A. Fokaides, S.A. Kalogirou, Application of infrared thermography for the determination of the overall heat transfer coefficient (*U*-value) in building envelopes, Applied Energy 88 (2011) 4358–4365.
[110] http://www.isover.com/Our-commitment-to-sustainability/Energy-efficiency/Energy-efficiency-in-buildings/Reducing-energy-consumption (Energy Efficiency in Buildings).
[111] R. Newport, Improving Electrical System Reliability with Infrared Thermography: Part 2. <http://www.electricity-today.com/et/june99/infrar.html>.
[112] J. Martinez, R. Lagioia, Experience performing infrared thermography in the maintenance of a distribution utility, in: 19th International Conference on Electricity Distribution: CIRED, 2007.
[113] ANSI/IEEE C37.010-4.4.3: IEEE Application Guide for AC High-Voltage Circuit Breakers Rated on a Symmetrical Current Basis.
[114] T.L. Hurley, Infrared techniques for electric utilities, in: X.P.V. Maldague (Ed.), Infrared Methodology and Technology, Gordon and Breach Science Publishers, Great Britain, 1994, pp. 265–317.
[115] R.A. Epperly, G.E. Heberlein, L.G. Eads, A tool for reliability and safety: predict and prevent equipment failures with thermography, in: Petroleum and Chemical Industry Conference, Banff, Alta, 1997, pp. 59–68.
[116] A. Showalter, J.S. Edmonds, In-service winding failure of newly installed replacement stator, in: International Conference on Electric Machine and Devices: IEMD 1999, Seattle, WA, 1999, pp. 797–799.
[117] M.J. Ralph, Power plant thermography – wide range of applications, in: Information Proceedings, 2004.
[118] J. Frate, D. Gagnon, R. Vilandre, R. Dansereau, Evaluation of overhead line and joint performance with high-definition thermography, in: IEEE International Conference on Transmission and Distribution Construction, Operation and Live-Line Maintenance, Montreal, Que, 2000, pp. 145–151.
[119] R.G. Bonin, Infrared reliability applications, in: Information Proceedings, 2005.
[120] B.H. Chudnovsky, Corrosion of electrical conductors in pulp and paper industrial applications, IEEE Transactions on Industry Applications 44 (2008) 932–939.
[121] W. Zhang, H. Peng, C. Su, Research on temperature variation of bridgewire with infrared thermal imaging, Advanced Materials Research 403–408 (2012) 675–679.
[122] M. Wang, A.J. Vandermaar, K.D. Srivastava, Review of condition assessment of power transformers in service, IEEE Electrical Insulation Magazine 18 (2002) 12–25.
[123] http://www.flir.com/cs/emea/en/view/?id=43622 (FLIR).
[124] N.P. Avdelidis, P.I. Nicholson, P. Wallace, Pulsed thermography in the investigation of PCBs for defect detection and analysis, in: 8th International Conference on Quantitative InfraRed Thermography, Padova, Italy, 2006.
[125] R.k. Vishwakarma, V. Mahule, M. Shahid, Fault diagnosing of a high density electronic card employing multiple power supplies using infrared thermography, Journal of Non destructive Testing and Evaluation 7 (2008) 28–31.
[126] P. Rodgers, V. Eveloy, J. Lohan, C.-M. Fager, P. Tiilikka, J. Rantala, Experimental validation of numerical heat transfer predictions for single- and multi-component printed circuit boards in natural convection environments, in: Proceedings of the 15th Annual IEEE Semiconductor Thermal Measurement and Management Symposium: SEMITHERM XV, San Diego, CA, USA, 1999, pp. 55–64.
[127] P. Rodgers, J. Lohan, V. Eveloy, C.-M. Fager, J. Rantala, Validating numerical predictions of component thermal interaction on electronic printed circuit

boards in forced convection airflows by experimental analysis, in: Proceedings of InterPACK'99: The PACIFIC RIM/International, Intersociety, Electronic Packaging Technical/Business Conference & Exhibition, Maui, Hawaii, USA, 1999.
[128] J. Lohan, P. Tiilikka, C.-M. Fager, J. Rantala, Effect of both PCB thermal conductivity and nature of forced convection environment on component operating temperature: experimental measurement and numerical prediction, in: Proceedings of the Sixteenth Annual Semiconductor Thermal Measurement and Management Symposium (SEMITHERM XVI), San Jose, CA, USA, 2000.
[129] B. Wiecek, E.D. Baetselier, G.D. Mey, Active thermography application for solder thickness measurement in surface mounted device technology, Microelectronics Journal 29 (1998) 223–228.
[130] A. Gupta, Y. Liu, N. Zamora, T. Paddock, Thermal imaging for detecting thermal interface issues in assembly and reliability stressing, in: 10th Intersociety Conference on Thermal and Thermomechanical Phenomena in Electronics Systems, ITHERM '06, San Diego, CA, USA, 2006.
[131] O. Breitenstein, M. Langenkamp, F. Altmann, D. Katzer, A. Lindner, H. Eggers, Microscopic lock-in thermography investigation of leakage sites in integrated circuits, Review of Scientific Instruments 71 (2000) 4155.
[132] H. Louche, A. Chrysochoos, Thermal and dissipative effects accompanying Luders band propagation, Material Science and Engineering A 307 (2001) 15–22.
[133] L. Wang, H. Zhang, Infrared information testing to the tensile necking-down phenomena of metal specimens, Applied Mechanics and Materials 94–96 (2011) 740–744.
[134] J.A. Rodriguez-Martinez, R. Pesci, A. Rusinek, Experimental study on the martensitic transformation in AISI 304 steel sheets subjected to tension under wide ranges of strain rate at room temperature, Materials Science and Engineering A 528 (2011) 5974–5982.
[135] W. Oliferuk, M. Maj, R. Litwinko, L. Urbanski, Thermomechanical coupling in the elastic regime and elasto-plastic transition during tension of austenitic steel, titanium and aluminium alloy at strain rates from 10^{-4} to 10^{-1} s^{-1}, European Journal of Mechanics A/Solids 35 (2012) 111–118.
[136] M. Kutin, Z. Adamovie, Tensile features of welded joint testing by thermography, Russian Journal of Nondestructive Testing 46 (2010) 386–393.
[137] N. Ranc, D. Wagner, Some aspects of Portevin–Le Chatelier plastic instabilities investigated by infrared pyrometry, Material Science and Engineering A 394 (2005) 87–95.
[138] H. Ait-Amokhtar, C. Fressengeas, Crossover from continuous to discontinuous propagation in the Portevin–Le Chatelier effect, Acta Materialia 58 (2010) 1342–1349.
[139] R. Peyroux, A. Chrysochoos, C. Licht, M. Lobel, Thermomechanical couplings and pseudoelasticity of shape memory alloys, International Journal of Engineering Science 36 (1998) 489–509.
[140] S.P. Gadaj, W.K. Nowacki, A.E. Pieczyska, Temperature evolution in deformed shape memory alloy, Infrared Physics & Technology 43 (2002) 151–155.
[141] D. Delpueyo, X. Balandraud, M. Grediac, Applying infrared thermography to analyse martensitic microstructures in a Cu–Al–Be shape-memory alloy subjected to a cyclic loading, Materials Science and Engineering A 528 (2011) 8249–8258.
[142] M. Wang, Y. Liao, D. Chen, Study on the thermal effects of rubbers during loading–unloading cycles by infrared thermography, Polymer Bulletin (2012) 1–10. http://dx.doi.org/10.1007/s00289-012-0795-x (23 June).
[143] M. Wang, Y. Liao, D. Chen, Study of the necking phenomenon in fiber drawing by infrared thermography, Polymer Testing 29 (2010) 674–678.
[144] C. Meola, G.M. Carlomagno, Impact damage in GFRP: new insights with infrared thermography, Composites Part A 41 (2010) 1839–1847.
[145] G. Fargione, A. Geraci, G.L. Rosa, A. Risitano, Rapid determination of the fatigue curve by the thermographic method, International Journal of Fatigue 24 (2002) 11–19.
[146] G.L. Rosa, A. Risitano, Thermographic methodology for rapid determination of the fatigue limit of materials and mechanical components, International Journal of Fatigue 22 (2000) 65–73.
[147] M. Naderi, A. Kahirdeh, M.M. Khonsari, Dissipated thermal energy and damage evolution of glass/epoxy using infrared thermography and acoustic emission, Composites Part B 43 (2012) 1613–1620.
[148] F. Maquin, F. Pierron, Heat dissipation measurements in low stress cyclic loading of metallic materials: from internal friction to micro-plasticity, Mechanics of Materials 41 (2009) 928–942.
[149] S. Giancane, A. Chrysochoos, V. Dattoma, B. Wattrisse, Deformation and dissipated energies for high cycle fatigue of 2024-T3 aluminium alloy, Theoretical and Applied Fracture Mechanics 52 (2009) 117–121.
[150] T. Ummenhofer, J. Medgenberg, On the use of infrared thermography for the analysis of fatigue damage processes in welded joints, International Journal of Fatigue 31 (2009) 130–137.
[151] A.E. Morabito, A. Chrysochoos, V. Dattoma, U. Galietti, Analysis of heat sources accompanying the fatigue of 2024 T3 aluminium alloys, International Journal of Fatigue 29 (2007) 977–984.
[152] O. Plekhov, T. Palin-Luc, N. Saintier, S. Uvarov, O. Naimark, Fatigue crack initiation and growth in a $^{35}CrMo_4$ steel investigated by infrared thermography, Fatigue and Fracture of Engineering Materials and Structures 28 (2005) 169–178.
[153] B. Yang, P.K. Liaw, H. Wang, J.Y. Huang, R.C. Kuo, J.G. Huang, Thermography: a new nondestructive evaluation method in fatigue damage, in: JOM-e: A Web-Only Supplement to JOM. <http://www.tms.org/pubs/journals/jom/0301/yang/yang-0301.html> (January, 2003).
[154] R.V. Williams, Monitoring the condition of machinery, Physics in Technology (1976) 166–171.
[155] J.K. Ghosh, S. Mukherjee, C. Ganguly, Infrared thermography for monitoring skin temperatures in inaccessible process plant equipment: case study, Quality Evaluation 9 (1989) 9–10.
[156] Z. Ge, X. Du, L. Yang, Y. Yang, Y. Li, Y. Jin, Performance monitoring of direct air-cooled power generating unit with infrared thermography, Applied Thermal Engineering 31 (2011) 418–424.
[157] R. Raistis, E. Jasiuiene, R. Sliteris, A. Vladisauskas, The review of non-destructive testing techniques suitable for inspection of the wind turbine blades, Ultragarsas 63 (2008) 26–30.
[158] S. Sheng, P. Veers, Wind turbine drivetrain condition monitoring – an overview, in: Applied Systems Health Management Conference, Virginia Beach, Virginia, 2011.
[159] F.P.G. Marquez, A.M. Tobias, J.M.P. Perez, M. Papaelias, Condition monitoring of wind turbines: techniques and methods, Renewable Energy 46 (2012) 169–178.
[160] A.G. Beattie, M. Rumsey, Non-destructive evaluation of wind turbine blades using an Infrared camera, in: 18th ASME wind energy Symposium, 37th Aerospace Sciences Meeting and Exhibit, Reno, NV, 1999.
[161] M.A. Drewry, G.A. Georgiou, A review of NDT techniques for wind turbines, Insight 49 (2007) 137–141.
[162] M.A. Rumsey, W. Musial, Application of infrared thermography nondestructive testing during wind turbine blade tests, Journal of Solar Energy Engineering 123 (2001) 271.
[163] H.-Y. Li, S.-M. Chao, G.-L. Tsai, Thermal performance measurement of heat sinks with confined impinging jet by infrared thermography, in: 16th International Symposium on Transport Phenomena: ISTP-16, Prague, 2005.
[164] J.-M. Karjanmaa, Thermal imaging and paper finishing machines, in: L.R. Allen (Ed.), Proceedings of SPIE: Thermosense XV, 1993, pp. 110–117.
[165] M. Fairlie, W. Fraser, B. Farahbakhsh, R. Lamb, O. Meijer, On-line temperature measurement in hot rolling of aluminum using infrared imaging system, in: G.B. McIntosh (Ed.), Proceedings of SPIE: Thermosense XI, 1989, pp. 84–92.
[166] M. Prystay, H. Wang, A. Garcia-Rejon, Application of thermographic temperature measurements in injection moulding and blow moulding of plastics, in: D.D. Burleigh, J.W. Spicer (Eds.), Proceedings of SPIE: Thermosense XVIII, 1996, pp. 5–14.
[167] A.G. Imgram, J.B. McCandless, Infrared thermal imaging of refinery equipment, in: G.E. Courville (Ed.), Proceedings of SPIE: Thermosense V, 1982, pp. 47–54.
[168] V. Leemans, M.-F. Destain, B. Kilundu, P. Dehombreux, Evaluation of the performance of infrared thermography for on-line condition monitoring of rotating machines, Engineering 3 (2011) 1030–1039.
[169] W. Kim, J. Seo, H. Yoon, N. Choi, D. Hong, Infrared thermographic diagnosis for fault detection of the bearings under stage of abrasion, in: 5th Pan American Conference for NDT, Cancun, Mexico, 2011.
[170] A. Mazioud, J.F. Durastanti, L. Ibos, E. Surugue, Y. Candu, Detection of rolling bearing degradation using infrared thermography, in: 9th International Conference on Quantitative Infrared Thermography, Krakow, Poland, 2008.
[171] H.A. Gaberson, Rotating machinery energy loss due to misalignment, in: Proceedings of the 31st Intersociety Energy Conversion Engineering Conference: IECEC 96, Washington, DC, 1996, pp. 1809–1812.
[172] G.H. Koch, M.P.H. Brongers, N.G. Thompson, Y.P. Virmani, J.H. Payer, Corrosion Costs and Preventive Strategies in the United States, Report by CC Technologies Laboratories, Inc. to Federal Highway Administration (FHWA), Office of Infrastructure Research and Development, Report FHWA-RD-01-156, September, 2011.
[173] E. Grinzato, V. Vavilov, Corrosion evaluation by thermal image processing and 3D modelling, Revue Générale de Thermique 37 (1998) 669–679.
[174] E. Grinzato, V. Vavilov, P.G. Bison, S. Marinetti, Hidden corrosion detection in thick metallic components by transient IR thermography, Infrared Physics & Technology 49 (2007) 234–238.
[175] S. Marinetti, V. Vavilov, IR thermographic detection and characterization of hidden corrosion in metals: general analysis, Corrosion Science 52 (2010) 865–872.
[176] J.-S. Han, J.-H. Park, Detection of corrosion steel under an organic coating by infrared photography, Corrosion Science 46 (2004) 787–793.
[177] M. Jonsson, B. Rendahl, I. Annergren, The use of infrared thermography in the corrosion science area, Materials and Corrosion 61 (2010) 961–965.
[178] A. Schonberger, S. Virtanen, V. Giese, H. Schrottner, C. Spieberger, Non-destructive detection of corrosion applied to steel and galvanized steel coated with organic paints by the pulsed phase thermography, Materials and Corrosion 63 (2012) 195–199.
[179] K.E. Cramer, P.A. Howell, H.I. Syed, Quantitative thermal imaging of aircraft structures, in: Proceedings of SPIE: Thermosense XVII, 1995, pp. 226–232.
[180] Z. Liu, M. Genest, D. Krys, Processing thermography images for pitting corrosion quantification on small diameter ductile iron pipe, NDT&E International 47 (2012) 105–115.
[181] V.P. Vavilov, E. Grintsato, P. Bizon, S. Marinetti, Detecting corrosion in steel products by dynamic infrared thermography, Russian Journal of Nondestructive Testing 30 (1994) 684–692.
[182] K.S. Hermanson, B.I. Sandor, Corrosion fatigue modelling via differential infrared thermography, Experimental Techniques (1998) 19–21.

[183] L. Chung, I.-K. Paik, S.-H. Cho, Y.-S. Roh, Infrared thermographic technique to measure corrosion in reinforcing bar, Key Engineering Materials 321–323 (2006) 821–824.
[184] G. Shen, T. Li, Infrared thermography for high-temperature pressure pipe, Insight 49 (2007) 151–153.
[185] P. Bison, M. Ceseri, G. Inglese, Mapping corrosion of metallic slab by thermography, Journal of Physics: Conference Series 214 (2010) 012073.
[186] J.M. Farley, J.L. Thompson, B.J. Dikstra, Nondestructive testing to avoid weld failures: a review, in: J.D. Harrison (Ed.), International Conference on Weld Failures, The Welding Institute, London, England, 1988.
[187] Y. Wang, B.A. Chin, On-line sensing of weld penetration using infrared thermography, Optical Techniques for Industrial Inspection 34 (1986) 314–320.
[188] W.H. Chen, B.A. Chin, Monitoring joint penetration using infrared sensing techniques, Welding Journal 69 (1990) 181s–185s.
[189] A.E. Bentley, S.J. Marburger, Arc welding penetration control using quantitative feedback theory, Welding Journal 71 (1992) 397s–405s.
[190] H.C. Wikle III, S. Kottilingam, R.H. Zee, B.A. Chin, Infrared sensing techniques for penetration depth control of the submerged arc welding process, Journal of Materials Processing Technology 113 (2001) 228–233.
[191] B. Grabas, J. Dard-Thuret, M. Laurent, Observation of penetration with infrared thermography in laser welding, Journal De Physique IV 4 (1994) 139–142. C4.
[192] B.A. Chin, N.H. Madsen, J.S. Goodling, Infrared thermography for sensing the arc welding process, Welding Journal 62 (1983) 227s–234s.
[193] M.A. Khan, N.H. Madsen, J.S. Goodling, B.A. Chin, Infrared themography as a control for the welding process, Optical Engineering 25 (1986) 799–805.
[194] S. Nagarajan, W.H. Chen, B.A. Chin, Infrared sensing for adaptive arc welding, Welding Journal 68 (1989) 462s–466s.
[195] C.C. Doumanidis, D.E. Hardt, Simultaneous in-process control of heat affected zone and cooling rate during arc welding, Welding Journal 69 (1990) 186s–196s.
[196] Y.-M. Kwak, C.C. Doumanidis, Geometry regulation of material deposition in near-net shape manufacturing by thermally scanned welding, Journal of Manufacturing Processes 4 (2002) 28–41.
[197] H.C. Wikle III, R.H. Zee, B.A. Chin, A sensing system for weld process control, Journal of Materials Processing Technology 89–90 (1999) 254–259.
[198] G. Bruggemann, A. Mahrle, T. Benziger, Comparison of experimental determined and numerical simulated temperature fields for quality assurance at laser beam welding of steels and aluminium alloyings, NDT&E International 33 (2000) 453–463.
[199] A. Lebar, M. Junkar, A. Poredos, M. Cvjeticanin, Method for online quality monitoring of AWJ cutting by infrared thermography, CIRP Journal of Manufacturing Science and Technology 2 (2010) 170–175.
[200] S. Lee, J. Nam, W. Hwang, J. Kim, B. Lee, A study on integrity assessment of the resistance spot weld by infrared thermography, Procedia Engineering 10 (2011) 1748–1753.
[201] C.C. Rusu, L.R. Mistodie, Thermography used in friction stir welding process, The Annals of 'Dunarea De Jos' university of Galati, Fascicle XII, Welding Equipment and Technology 21 (2010) 62–66.
[202] B. Venkatraman, M. Menaka, M. Vasudevan, B. Raj, Thermography for online detection of incomplete penetration and penetration depth estimation, in: 12th Asia–Pacific Conference on NDT Auckland, New Zealand, 2006.
[203] M. Speka, S. Mattei, M. Pilloz, M. Ilie, The infrared thermography control of the laser welding of amorphous polymers, NDT&E International 41 (2008) 178–183.
[204] C. Ganne-Chedeville, M. Properzi, A. Pizzi, J.-M. Leban, F. Pichelin, Parameters of wood welding: a study with infrared thermography, Holzforschung 60 (2006) 434–438.
[205] N.M. Nandhitha, N. Manoharan, B.S. Rani, B. Venkatraman, P. Kalyansundaram, B. Raj, Comparative study on the suitability of feature extraction techniques for tungsten inclusion and hotspot detection from weld thermographs for on-line weld monitoring, Indian Journal of Engineering & Materials Science 17 (2010) 20–26.
[206] US Department of Energy, David Gleaton, Infrared Thermography at the Savannah River Site. <http://www.osti.gov/bridge>.
[207] R. Lewak, Infrared techniques in the nuclear power industry, in: X.P.V. Maldague (Ed.), Infrared Methodology and Technology, Gordon and Breach Science Publishers, Great Britain, 1994, pp. 319–366.
[208] P. Rodriguez, B. Raj, Development of in-service inspection techniques for nuclear power plants in India, International Journal of Pressure Vessels and Piping 73 (1997) 59–68.
[209] S.G. Lee, W.T. Kim, Inspection of the leakage for the closure plug of heavy water reactor using infrared thermography in nuclear on-site application, in: 10th International Conference on Quantitative InfraRed Thermography, Quebec, Canada, 2010.
[210] W. Kim, H. Park, M. Choi, S. Lee, B. Lee, J. Kim, D. Hong, Detection of piping defects in nuclear plants by ultrasonic pulse-phase thermography, in: 10th European Conference on Nondestructive Testing: ECNDT 2010, Moscow, Russia, 2010.
[211] F.J. Madruga, D.A. Gonzalez, J.M. Mirapeix, J.M.L. Higuera, Application of infrared thermography to the fabrication process of nuclear fuel containers, NDT&E International 38 (2005) 397–401.
[212] B. Venkatraman, M. Menaka, P. Kalyanasundram, B. Raj, Infrared imaging – an overview on ITSS multifarious possibilities and applications in IGCAR, Journal of Non-destructing Testing & Evaluation 5 (2006) 54–67.
[213] X. Courtois, A. Durocher, M. Lipa, Health monitoring of Tore-Supra Toroidal Pump Limiter using Lock-in thermography, Fusion Engineering and Design 84 (2009) 628–631.
[214] A. Durocher, F. Escourbiac, M. Richou, N. Vignal, M. Merola, B. Riccardi, V. Cantone, S. Constans, Infrared thermography inspection of the ITER vertical target qualification prototypes manufactured by European industry using SATIR, Fusion Engineering and Design 84 (2009) 314–318.
[215] E. Gauthier, H. Roche, E. Thomas, S. Droineau, B. Bertrand, J.B. Migozzi, W. Vliegenthart, L. Dague, P. Andrew, T. Tiscornia, D. Sands, ITER-like wide-angle infrared thermography and visible observation diagnostic using reflective optics, Fusion Engineering and Design 82 (2007) 1335–1340.
[216] E. Saarimaki, P. Ylinen, An investigation of non-destructive thermographic inspection exploiting phase transition of water for moisture detection in aircraft structures in: 9th International Conference on Quantitative InfraRed Thermography, Krakow, Poland, 2008.
[217] C. Ibarra-Castanedo, M. Genest, S. Guibert, J.-M. Piau, X.P.V. Maldague, A. Bendada, Inspection of aerospace materials by pulsed thermography, lock-in thermography and vibrothermography: a comparative study, in: Proc. SPIE 6541, Thermosense XXIX, 2007.
[218] C. Meola, G.M. Carlomagno, A. Squillace, A. Vitiello, Non-destructive evaluation of aerospace materials with lock-in thermography, Engineering Failure Analysis 13 (2006) 380–388.
[219] T. Schmidt, S. Dutta, T. Ullmann, Production integrated NDT by means of automated thermography in: 11th International Conference on Quantitative Infrared Thermography, Naples, Italy, 2012.
[220] D.S. Burleigh, Infrared techniques in the aerospace industry, in: X.P.V. Maldague (Ed.), Infrared Methodology and Technology, Gordon and Breach Science Publishers, Great Britain, 1994, pp. 429–452.
[221] C. Meola, G.M. Carlomagno, Recent advances in the use of infrared thermography, Measurement Science & Technology 15 (2004) R27–R58.
[222] http://www.infratec.de/en/thermography/application-area/process-optimisation/aviation.html.
[223] E.A. Veraverbeke, P. Verboven, J. Lammertyn, P. Cronje, J.D. Baerdemaeker, B.M. Nicolai, Thermographic surface quality evaluation of apple, Journal of Food Engineering 77 (2006) 162–168.
[224] P.J. Fito, M.D. Ortola, R.D.l. Reyes, P. Fito, E.D.l. Reyes, Control of citrus surface drying by image analysis of infrared thermography, Journal of Food Engineering 61 (2004) 287–290.
[225] L.N. Costa, C. Stelletta, C. Cannizzo, M. Gianesella, D.P.L. Fiego, M. Morgante, The use of thermography on the slaughter-line for the assessment of pork and raw ham quality, Italian Journal of Animal Science 6 (2007) 704–706.
[226] J.H. Song, S. Shida, Infrared thermography for monitoring surface checking for wood during drying, in: 11th International IUFRO Wood Drying Conference, Skelleftea, Sweden, 2010.
[227] C.C. Plescanu, M. Klein, C. Ibarra-Castanedo, A. Bendada, X. Maldague, Localization of wood floor structure by infrared thermography, in: Proc. of SPIE: Thermosense XXX, 2008, pp. 693911.
[228] V. Pasagic, M. Muzevic, D. Kelenc, Infrared thermography in marine applications, Brodogradnja 59 (2008) 123–130.